Ocean Forecasting: From Regional to Coastal Scales

Emil V. Stanev[1], Johannes Schulz-Stellenfleth[1], Joanna Staneva[1], Sebastian Grayek[1], Sebastian Grashorn[1], Arno Behrens[1], Wolfgang Koch[1], Johannes Pein[1]

5

[1]Institute of Coastal Research, Helmholtz-Zentrum Geesthacht, Geesthacht, 21502, Germany

Correspondence to: Emil V. Stanev (emil.stanev@hzg.de)

Abstract. In the past years, the Helmholtz Zentrum Geesthacht put in place the Coastal Observing System for the North and Arctic Seas (COSYNA) in the frame of which different aspects of forecasting the marine environment have been developed.
10 This paper describes these developments, which are based on recent advances in coastal ocean forecasting in the field of numerical modelling, data assimilation and observational array design. The region of interest is the North and Baltic Sea; most of the coastal examples discussed in the paper are for the German Bight. Several pre-operational applications are presented exemplifying the outcome of using the best available science in coastal ocean predictions. They help to identify new challenges; most of them are associated with resolving the non-linear behavior of coastal ocean, which for the studied
15 region, is manifested by the tidal distortion and generation of shallow-water tides. Led by the motivation to maximize the benefit from observations, the authors focus on the integration of observations and modelling by using advanced statistical methods. The coastal and regional ocean forecasting systems do not run in isolation, but are linked, either weakly by just using forcing data, or interactively by using two-way nesting or unstructured-grid models. Therefore the problem of downscaling and upscaling, which currently attracts much attention, is also addressed. One example shown is the coupling of
20 the coarse-resolution regional models by using a two-way nesting method with fine resolution in the area of connecting straits. The major part of the paper presents illustrations from assimilation of remote sensing, *in situ* and HF radar data, prediction of wind waves and storm surges, as well as possible applications to search and rescue operations, and modelling support for assessing the environmental impact of wind parks. Concepts for seamless approaches to link coastal and regional forecasting systems are also presented and the two examples given illustrate (1) an application of unstructured-grid model
25 for the Ems Estuary, and (2) the potential influence of the information from coastal observatories or coastal forecasting systems on the regional models.

1 Introduction

Science developments are in the heart of newly emerging coastal ocean services supporting the blue and green growth (She et al., 2016). Although the volume of coastal ocean observations around Europe is big in comparison to the open-ocean ones, they alone are not enough to fully support the present-day needs for high-quality ocean-forecasting and monitoring. Recent

5   practices in this field are based not only on observations, but use widely numerical modelling. Numerous integrated coastal observing and modelling systems are providing not only services, but also research advancement. Internationally recognized examples of integrated systems are described by Kourafalou et al. (2015a), while the advancements of coastal ocean forecasting are reviewed by Kourafalou et al. (2015b). Many individual institutes develop their ocean monitoring and forecasting activities both in the open and coastal oceans (one recent example is presented by Siddorn et al., 2016). The new

10   challenges and trends in this field were recently reviewed by She et al. (2016).

In the present study the focus is on similar developments in the area of the German Bight. We will present some research issues relevant to the pre-operational oceanography. The link to the operational forecasting (e.g., forecasting which is performed by the authorized state agencies, one such is the German Federal Maritime and Hydrographic Agency known as

15   the Bundesamt für Seeschifffahrt und Hydrographie, BSH) will be limited in the present study to using data from operational models for analyses and inter-comparisons. Skill estimates have been considered in earlier publications, where more details are given about the systems' performance.

The North and Baltic Seas (Fig. 1), which are among the best-studied coastal areas in the world ocean, are also playgrounds

20   for intensive marine use and various activities. This could create possible conflicts and at the same time attract a wide social, economic and political attention. One extreme event, which streamlined the societal concern was the Great Flood of 1962, during which 315 people in Hamburg and another 35 in the rest of northern Germany died. Because of the measures, which have been taken afterwards, including modern prediction and warning systems, similar devastations never happened again.

25   The need to solving a number of practical problems motivates a serious consideration of the usefulness of coastal research (Storch et al., 2015). One basic issue to be answered when estimating the efficiency of the present-day coastal forecasting systems is how well these systems benefit from the available data (Kourafalou et al, 2014a, b). Therefore, we define the main goal of this paper as to showcase methodologies integrating observations and models in coastal areas. Analysis of the synergy of coastal and larger-scale forecasting systems is our second goal.

30

The coastal ocean integrated forecasting systems enable monitoring and predictions of the coastal ocean state by appropriately accounting for the dominant coastal processes at a wide range of characteristic scales ranging from sub-mesoscale to regional-basin scales. Of big importance are the exchanges along and across the shelf break, storm surges, tides, internal waves, surface waves, fronts, slope currents, estuarine processes, river plumes and suspended sediment dynamics. Close to the coast biogeochemical processes show large diversity and strong gradients. Possible environmental consequences associated with the transport and accumulation of matter and pollutants necessitate that predictions are characterized by high confidence and timeliness. The challenge is to use multidisciplinary and multiscale observations, as well as seamless modelling suite with interacting modules well representing the individual sub-systems: atmosphere, waves, circulation, biogeochemistry. Adding to the forecasting suite atmospheric and wave models is strongly needed because the air-sea interaction can be well traced down to the shallow bottom. This specific case differs largely from the known case in the open-ocean where the coupling between bottom layer and atmosphere is less direct.

The challenge in data assimilation is to extract the most important information from relatively sparse and noisy observations, and to feed this information in an optimal way into numerical forecast models. The observation errors are due to instrumental noise, sampling, and possible misinterpretation of measurements. Numerical ocean models are obviously also not error-free; errors are originating from the incomplete (non-perfect) model physics, insufficient grid resolution, problems in open boundary conditions, atmospheric or hydrological forcing. Even "perfect" ocean models will drift away from the reality, which is known as loss of predictability beyond the predictability limit. This limit depends upon the geophysical processes. For the synoptic processes in the open-ocean this time is of the order of weeks to months, for the coastal ocean it is of the order of hours and days. The loss of predictability (short memory of coastal systems) is associated with the nonlinear transfer and growth of errors. The consideration of these non-linear effects, which is one of the major subjects in the present study, is addressed by investigating the relationship between astronomical and shallow-water tides.

Because the data problematics is addressed in more detail in other papers in this special collection we will restrict our analysis mostly on numerical modelling, data assimilation, coupled models and seamless modelling in the coastal area. The part dealing with numerical modelling will describe the used models. Data assimilation will be illustrated using the example of assimilating HF radar and some other data with a focus on the intra-tidal processes. Forecast-uncertainty will also be addressed in this part. Coupled modelling will be illustrated based on the example of coupling circulation and wind wave models. Short conclusions and outlook will be given at the end.

2 Numerical models

2.1 Coastal-ocean modelling and forecasting

Open-ocean and coastal ocean modelling have many similarities but also substantial differences. Not only are the research questions different, but also the demand for specific characteristics of forecasting. In particular, the resolution of fine spatial scales and high frequencies imposes difficult requirements. While most of the volume of open-ocean is characterized by a low level of turbulence, the coastal ocean is an essentially dissipative system. Therefore, a more complete representation of the turbulence production and dissipation are needed along with a deeper knowledge of their temporal and spatial dynamics. The small scales processes, which are dominant in the coastal ocean, call for a deeper consideration of mesoscale to sub-mesoscale dynamics and their interplay with the larger-scale processes. Of particular importance is the improvement in the description of exchanges between the coastal and open-ocean, as well as its coupling with estuaries and catchment areas.

The specificities in the coastal ocean make it crucial that numerical models develop a resolution capacity compliant with the dominant spatial scales. Furthermore, the theoretical developments need to be consistent with the technological advancements in the field of sensors and new observational platforms (e.g., high-resolution wide-swath altimetry, geostationary sensors). One challenging perspective is to linking the coastal forecasting to surface currents directly estimated from satellites, high resolution SST, etc. As a response to these challenges specific aspects of modelling need to be improved/enhanced. Among the most important developments needed to be further advanced are the seamless modelling, coupling of coastal models with atmospheric and surface wave models, as well as further development of the biogeochemistry and morphodynamic models. In addition, more flexible coupling is needed between regional and coastal models, including estuarine models. Advanced numerical schemes and parameterizations are required for numerical codes, in particular for seamless ones enabling to simultaneously and adequately resolve multi-scale interactions (Zhang et al., 2016). The development of flexible interfaces to couple structured and unstructured grids is also needed along with more advanced understanding of the fact that the coupling is not one-way, because the propagation of information is essentially in two ways.

On the road of improvement of model performance the multi-model approach (Golbeck et al., 2015) gains more importance, however the model inter-comparison needs further focusing on physical representativeness; the comparison with data has to be further deepened using coastally-tailored methods and metrics. Although many developments exist in the North Sea resolving high-frequency processes (e.g., tides), tidally relevant metrics seem not to be used in model inter-comparisons sufficiently enough.

2.2 Model inter-comparison. Focus on tides

2.2.1 Astronomic and shallow-water tides

The tidal dynamics in the deep ocean are almost linear and using a number of constituents adequately describes the tide. As demonstrated by Shum et al. (1997) global ocean tide models in the deep ocean agree within 2-3 cm. In shallow water the tidal dynamics is nonlinear and the nonlinear distortion causes compound and over-tides to appear. The nonlinearities are due to the quadratic bottom friction and advection term (Le Provost, 1991). The latter generates over-tides (M4) of twice the

5   frequency of the astronomic M2 tide. The friction term is responsible for the generation of the odd harmonics (e.g., M6). These shallow-water tides are very important for the tidal dynamics in some coastal areas. Southwest of Britain and in the Irish Sea their amplitude is comparable with the amplitude of M2 tide (Andersen, 1999). As it has been recently demonstrated by Stanev et al. (2015), the M4 tides in the German Bight cause a strong tidal asymmetry. The need for increasing accuracy of tidal predictions in the shelf regions makes it mandatory to account for the higher harmonics and

10   evaluate the capabilities of ocean tide models to resolve them.

Knowing the high accuracy of satellite altimetry in the open-ocean one could expect that it can be considered as a strong "competitor" of coastal tidal models. However, the real situation is such that, on the continental shelves, coastal models seem to perform better than the global ones, however the altimeter data close to the coasts are less accurate than the open-ocean

15   ones. In these coastal areas the tidal range is usually larger than in the open-ocean, and the propagation of tidal waves is more complex because of numerous factors (two of them are the strongly variable bottom friction and vertical stratification in the regions of fresh-water influence, ROFIs). Furthermore, higher tidal harmonics are difficult to be measured from satellites (Andersen, 1999). Thus, one natural step for the future is to investigate the adequacy of altimeter data and numerical simulations in the coastal ocean. Further steps would suggest using data-assimilation methods to supplement

20   hydrodynamic models (Andersen et al., 2006; Egbert et al., 2010; Schulz-Stellenfleth and Stanev, 2016).

2.2.2 The rationale of inter-comparison

Although some steps have already been done in the field of the North Sea model inter-comparisons (e. g., one model against another model, see Stips et al., 2006; Su et al., 2025), there is still a demand to (1) compare more than two models operating

25   in the same area (Golbeck et al., 2015), (2) consider metrics appropriate for the North Sea, and (3) address both model-to-model inter-comparison in parallel with model versus data comparison. Because no much attention has been given in the past to the performance of simulations to resolve the tidal variability of the baroclinic North Sea, and because the predictions in wide coastal areas have a large practical value (e. g., small errors in tidal phase can largely impact the success of search and rescue operations, SAR), we will present one example below. The models and their set ups, which are used in the inter-

30   comparison are briefly presented in the Annex. These models are the following: Nucleus for European Modelling of the Ocean (NEMO, two setups, of which one is operational), General Estuarine Transport Model (GETM), the operational model of BSH (BSHcmod, two setups, of which one is operational), and the Semi-implicit Cross-scale Hydroscience Integrated System Model (SCHISM). These models (see Annex 6) are central or related to all applications discussed in the present work therefore a critical examination of their capabilities to reproduce dominant characteristics of dynamics is

needed. Because the tidal forcing is the most important one in the North Sea with respect to the amount of mechanical energy provided, we will focus in the following on the capabilities of different models to adequately simulate tides.

The inter-comparison addressed here is only illustrative and a more complete study is underway. As an example, we will
5 focus on M2 and M4 tides, which are of high theoretical and practical relevance. It has to be kept in mind that the models presented above differ not only because the used numerics are different. They have different resolution in the vertical and horizontal, different topography, different boundaries, as well as different forcing. The coastal line, which is the same for all models in their overlapping areas, is differently resolved in the individual models.

10 One part of the numerical simulations presented below is carried out in the frame of the present study. The results from another two models are presented using freely available data from operational agencies. Because model setups differ it is not possible to objectively identify the strengths and weaknesses of different models, and this is not our aim. We rather addresses the question of how several, relatively similar, numerical simulations compare with each other.

15 As far as the comparison between numerical simulations and observations is concerned, this has already been initiated by Andersen (1999), who compared the over-tides estimated from altimeter data and the ones simulated by the model of Flather (1976; 1981). Unlike to that work we will concentrate on the representation of M4 tide by several models described in the Annex. This is of utmost importance for the coastal modelling, because it gives a good illustration of possible problems associated with non-linear processes, which many models do not well simulate.

20

2.2.3 M2 tides

With the pioneering work of Praudman and Doodson (1924) and many other authors in the 20th century the knowledge about the tidal dynamics in the North Sea reached a very mature status in comparison to other ocean areas. This is also due to the fact that the north-western European shelf is the most intensively surveyed ocean area in the world, as far as tidal data is
25 concerned. According to Andersen (1999) a total of 270 coastal and pelagic tide gauges were available on the shelf.

The M2 tide, which is essentially a Kelvin wave, is reproduced in a very similar way by all models (Fig. 2a). All tidal analyses presented in this figure compare well with a numerous earlier numerical simulations cited above, as well as with the satellite observations (Woodworth and Thomas, 1990). The highest M2 amplitudes appear in the English Channel. Large
30 magnitudes are also simulated in the German Bight; the values simulated in GETM in this area being lower than in the other models.

There are four M2 amphidromic points in the studied model area. The one in the English Channel is close to the British coast, as known from the earlier analyses (Chabert d'Hières and Le Provost, 1970). The amphydromic point between the

British Isles and the Netherlands's coast is at the same location in all models. Small differences between the NEMO simulations and the simulations by the remaining models can be found in the area around the German Bight amphidromy. This is attributed to the fact that the minimum depth in the two NEMO models along the coast is approximately eight meters, which is deeper than in the other models.

5

The closed boundary in the Danish Straits in the FOAM-AMM7 (this model is run only for the North-west shelf) results in a generation of an amphidromic point in the Kattegat. In all other (coupled with the Baltic Sea models) the amplitude of M2 continuously decreases with approaching the Danish straits. This demonstrates how important is to have the North and Baltic Sea models coupled.

10

It is known that the amphidromic point in front of the Norwegian coast is not simulated in an identical way in other simulations reported in literature. This is also the case in our inter-comparison, in which the M2 phase-pattern is shifted to the East, such that an amphydromic point cannot longer be observed in the ocean (BSHcmod and GETM). This amphidromic point is in the ocean in the two NEMO setups and on the coast in SCHISM. The most appropriate candidate explaining these differences is the bathymetry and the resolution of coastal line (the most adequate is the resolution in SCHISM).

15

2.2.4 Shallow water tides

The North Sea shallow water tides (e. g., M4 and M6) have small amplitudes compared to M2 tide, also in the shelf regions (Fig. 2b). The fact that they are not well resolved by the numerical models and observations could explain the limited knowledge about the spatial patterns of these harmonics in the past. However, most coastal processes are crucially dependent on the tidal asymmetry, which is determined by the relationship between the amplitude and phase characteristics of over tides and astronomical tides. The comparison between amplitudes of the individual constituents (not shown here) indicates that by far the most important of the nonlinear tides is the M4 one. One area where the over-tides are clearly not small is the English Channel (Chabert d'Hières and LeProvost, 1970; Andersen et al., 2006), which is supported by the results of all models (Fig. 2b).

M4-tide amplitudes show very complex patterns and some pronounced differences in all models (Fig. 2b). This is just one demonstration of how different the representation of the non-linearities in the analyzed models is. However, there are a number of features, which are similarly represented in all models. In comparison to the M2 tidal properties, the ones of M4 tides have smaller scales (see Stanev et al., 2015 for the explanation of this). Among the similarities between the different models we will mention the following. A large-scale minimum is simulated in the northern (open-ocean part) of all models. Two minima of M4 amplitude are simulated in the English Channel in all models with slight difference in their position and extension. The low M4-magnitude area in front of the Elbe and Weser estuaries (known from the analyses of Stanev et al.,

2015) is simulated in a qualitatively similar way by all models, however its position is slightly different in all models. Good agreements also exist between the simulated amplification of M4 amplitude in the embayments along the British coast. The two simulations by BSHcmod are almost identical because the two models and their setups are very similar.

One obvious difference between the individual simulations is the representation of the "wavy"- patterns along the southern coast, which is weaker in FOAM-AMM7. However, the overall agreement between the simulations in Fig. 2b and the satellite observations (see Plates 1, 2 in Andersen (1999)) seems reasonable. In particular it appears that all models addressed here are superior with respect to the relatively old hydrodynamic shelf model of Flather (1976; 1981) used by these authors. Unlike the good agreement between the M2 phases simulated by all models, the phases of shallow-water tides differ substantially. Because these phases are very important for the tidal asymmetry of the coastal ocean dynamics, further attention is needed with respect to the performances of regional models in the coastal ocean. The results of Stanev et al. (2015) give a plausible explanation of the above problem. With the exception of SCHISM, all other considered models using coarse resolution of several kilometers, simulate very differently (and perhaps not adequately enough) the tidal dynamics, and in particular the distortion of tidal signal in the shallow coastal zone of the North Sea.

In conclusion of this part we stress that as far as the astronomical tides are concerned the quality of the present-day simulations based on regional models seems good. However, the quality of the regional models with respect to the over-tides needs further attention, in particular when developing coastal applications. This is the reason why the cases considered in Sect. 3 and 4 are focused on the German Bight only or even on smaller areas, where the fine resolution used enables more adequate simulations in the coastal zone. It is desirable that further model inter-comparisons have to be extended towards more quantitative-like estimates based on the present-day available data from remote sensing and tidal gauges.

2.3 Two-way nested NEMO

The Danish Straits are of fundamental importance for the exchange between the North Sea and the Baltic Sea (Sayin and Krauß, 1996), providing a major control for the Baltic Sea stratification (see, e. g., Meier and Kauker, 2003; Döos et al., 2004; Feistel et al,, 2006, and the references therein). The commonly used approaches to deal with the complex Danish Straits' bathymetry in the nested numerical simulations are addressed by She et al. (2007), along with the influence of bathymetry on the salt- and freshwater flow-rates. In that work the model setup, which was based on the BSHcmod, used 50 z-levels with a resolution of 4 nm for the North Sea and Baltic Sea. A fine resolution model was nested in an area covering the Danish Straits, which had 25 z-levels and 1 nm horizontal resolution. However, this and other previous studies did not address in detail the nesting procedures and technicalities, which have to be applied to the transition area between the North Sea and Baltic Sea in order to adequately resolve the water and salinity exchange. One solution would be to use the standard two-way grid refinement tool for the NEMO framework (e. g., AGRIF, Adaptive Grid Refinement in FORTRAN).

Existing practices demonstrate that this is an effective tool for the horizontal grid refinement (see, e. g., Laurent et al., 2005; Cailleau et al., 2008; Jouanno et al., 2008). However, to our knowledge no applications for the vertical grid refinement exist.

Below the performance of a new two-way nesting method (Grayek and Stanev, paper in preparation) enabling the usage of different vertical discretization in the individual nests of the North Sea-Baltic Sea NEMO is presented. The use of different vertical grid types (σ-levels and z-levels) in the different parts of the nested models is proposed as a step forward in comparison to the system described by She et al. (2007). The configuration includes three nested areas: one for the North Sea (red and green areas in Fig. 3a), one for the Baltic Sea (green and blue areas) and one for the Danish Straits (the green area in Fig. 3a). Thus, the North Sea and Baltic Sea models overlap over the transition area between the two seas. The horizontal resolution for the North Sea and the Baltic Sea models is 2 nm. In the vertical the North Sea model uses 21 σ-levels. The Baltic Sea model uses 35 z-levels in the vertical. This choice has been made in order to avoid possible problems due to pressure gradient errors in terrain-following coordinate systems.

The two coarse resolution models exchange boundary conditions at their outer open boundaries. At the Baltic Sea boundary the North Sea model uses boundary forcing provided by the Baltic Sea model, which are interpolated onto the North Sea grid. In the same way, the Baltic Sea model receives boundary forcing data at its western boundary from the North Sea model. The first two panels in Fig 3c show the simulated salinity and currents along the transect-line shown in Fig. 3b. As expected the representation of the dynamics in the transition zone as seen by the two models is not identical, the z-level model (the Baltic Sea one) reproduces clearly the estuarine circulation in the straits, while the σ-level one (the North Sea) reveals much weaker stratification. Remember that the physical parameterizations in the two models are the same.

It is not only the vertical resolution, which affects the model-performance, but also the horizontal resolution in the straits. Therefore another simulation was performed, in which the interplay between the North Sea and Baltic Sea models was different: (1) data were exchanged not only via the open boundaries (as in the case considered above), and (2) a Danish Straits model with a finer spatial resolution of 0.5 nm in the horizontal and 35 terrain-following σ-levels in the vertical is used. The proposed method distinguishes between 'parent' and 'child' nests or models. The child nest (the Danish Straits model) receives its boundary forcing from is the parent nests (the North Sea and the Baltic Sea models). In the following "assimilation"-step the child model "exports its data onto the overlapping area of the two parent models using a data-assimilation approach. This second step explains the main difference between the proposed nesting and the classical method. The difference is the handling of the information flow from the child to the parent nests, which enables a gradual up-scaling (see also Schulz-Stellenfleth and Stanev (2016)), while at the same time maintaining the overall dynamical consistency of the parent nest. Another basic difference to the existing practices is that the "child-nest" has "two parents", in our case the North Sea (red and green) and Baltic Sea (green and blue) models, which do not directly communicate one with another.

This technique appeared capable to avoid problems with simulating the M2 tide in the Kattegat, as it was the case with the FOAM-AMM7, which is operated only for the North Sea (see Fig. 2a).

The different models are synchronized in the following way: The coarse resolution model runs are segmented in a one day hindcast and a one day forecast phase. During the hindcast phase the coarse resolution models receive the enhanced fine resolution information over the whole domain of the fine grid. During the forecast phase of the coarse resolution model no nudging is applied and the models run in a free prognostic mode. In the next cycle of the coupling procedure the fine resolution model is re-run for the whole hindcast-forecast period of the coarse resolution models using interpolated coarse resolution output as boundary condition.

The bottom two panels of Fig. 3c depict the simulated salinity and velocity fields from the two Baltic Sea parents and child runs during a small inflow event on September 16th, 2010. The first one illustrates how the Baltic "parent" sees the transition zone; the second illustrates how the "child"-nest sees it. Because of this specific nesting the Baltic Sea "parent" got some features from the North Sea counterpart via the "child" model (see the third plot in Fig. 3c). The fine resolution nest shows some displacement of the estuarine front and an increased bottom salinity in the vicinity of the Darss Sill (at approximately 80% of the transect length) and thus an increased stratification.

The differences between individual simulations can be explained by the changes in the secondary circulation (Fig. 3d) resulting in a stronger vertical current component, which brings up saltier water originating from the Kattegat (between approximately 10% and 45% of the transect length). These subtle processes present a real challenge to be simulated on a coarser-resolution grid. Although the overall salinity and current patterns along the cross section are comparable in the two simulations (Fig. 3c) the salinity transport along the track deviates significantly in different models. Comparing the "Baltic Sea parent (z-level;coarse)" with the "Baltic Sea parent (z-level; coarse) + assimilation" (the third and fourth plots in Fig. 3c) shows that the proposed procedure helps to reduce this deficiency without any negative impact on the consistency in the coarse resolution simulation.

3 Data assimilation

3.1 Data assimilation in the coastal ocean

During the last years ocean data assimilation and forecasting has reached an impressive level of maturity (Chasignet and Verron, 2006). One good example is the Global Ocean Data Assimilation Experiment (GODAE), where several systems have been developed and are operated by the Australian Bureau of Meteorology (BLUElink Ocean Data Assimilation System, BODAS), the Jet Propulsion Laboratory (Estimating the Circulation and Climate of the Ocean, ECCO), the UK Met Office (Forecast Ocean Assimilation Model, FOAM), other Copernicus systems based on the NEMO VARiational data

assimilation (NEMOVAR), and some others (Cummings et al., 2009). These GODAE systems assimilate various measurements such as sea level anomaly data provided by satellite altimeters, subsurface temperature and salinity data from Argo floats, moored and drifting buoys, expendable bathythermograph (XBT), and conductivity-temperature-depth (CTD) recorders, in situ and satellite sea surface temperature data, as well as satellite derived sea ice concentration and drift data.

5

So far ocean data assimilation techniques have been applied for operational forecasts, error analysis, parameter optimization, for ocean process studies, and observational network design. Compared to the methodologies used in meteorology and global oceanography, coastal forecasting techniques are still at a relatively early stage of development. This is because the specific problems of ocean data assimilation in coastal ocean are full of challenges, which are not sufficiently addressed in global or

10 regional ocean data assimilation. This motivates us to formulate below some specific coastal problems and illustrate solutions of some of them.

Complexity of data assimilation in the coastal ocean increases with the vast range of phenomena and the multitude of interactive scales in space and time (DeMey et al., 2009; De Mey and Proctor, 2009, Korres et al., 2012). The spatial and

15 temporal resolution required for realistic coastal predictions is much higher than the resolution required for the deep ocean. Processes, which are sometimes disregarded in the open-ocean data assimilation, such as tides and the high-frequency barotropic response to atmospheric forcing, become dominant in the coastal ocean. The small temporal scales (hours) and horizontal scales (hundreds of meters) are both computationally and scientifically challenging for data assimilation.

20 The diversity of methods used to assimilate data in coastal models reflects the complexity of coastal processes and the status of forecasting systems, which are still dealing with research issues. Efforts are however underway to test and improve quality of data assimilation in operational practices, one example for the region addressed here is given by Stanev et al. (2011).

Several problems associated with coastal data assimilation are listed below.

25 1. *The variables of interest* for coastal applications include the same physical properties as in the open-ocean models, but also near bottom currents, which are important for sediment transport and a large number of biogeochemical properties. This greatly increases the number of variables and the complexity of models and the assimilation schemes. Short time scales (e.g., minutes to hours for tides) increase not only the demand for high-quality observations, but also for specific data assimilation schemes.

30 2. *Vigorous adjustment process* arises in sequential data assimilation, when they are restarted (e.g., Malanotte-Rizzoli et al., 1989). A too frequent assimilation of observations can even lead to the situation, where the assimilation degrades the model results due to the high-frequency perturbations generated by the assimilation (Talagrand, 1972). One approach to overcome this problem will be illustrated in the following sections.

3. *The data and observational platforms* differ from the ones in the open ocean. For example, satellite altimetry does not fully resolve all important coastal-ocean scales; data from profiling floats are not available in the shelf seas. However, data from high-frequency (HF) radars and ADCP, sea level from coastal tide gauges and bottom pressure gauges, water properties from fixed data stations and ferries, gliders, and AUVs gives new perspectives. In particular, the assimilation of altimetric data must also account for the aliasing of the tidal signal, which can well be compensated by using the synergy between altimeter, tide gauge and HF radar data.

4. *The complex physics* in the coastal zone complicates the assimilation of data and necessitates resolving the whole spectrum of free-surface variations (tides, storm surges), multiple scales, friction and mixing effects and associated tidal straining and fronts, dependency of solution of small-scale bathymetric channels and variations of bathymetry (which is not well known, see Jacob et al., 2016), control of straits for the inter-basin exchange and inlets for the exchange between tidal flats and open ocean, drying and flooding. The situation is further complicated by the complex nonlinear processes (e.g., creation of over-tides), strong coupling of the variability at different frequencies, and relatively "short memory" of the physical processes.

5. *The observation error specification* is extremely challenging in the coastal zone; specific costal processes necessitate using dynamically-consistent error prediction schemes (Stanev et al., 2015). Most of the existing assimilation schemes assume unbiased observations with Gaussian noise, which is often unrealistic. For many coastal observational platforms the determination of errors is difficult also because some platforms, e.g., satellite altimeters, show larger errors in the coastal zone.

6. *Coupling coastal and deep ocean models* is still not a well-solved problem. Most coastal models are one-way nested; the model solution is strongly controlled by boundary forcing originating from larger-scale models. Two-way nested models enable that (assimilated) information from coastal observations, which is usually not assimilated by the larger-scale forecasting systems, is propagated out of the coastal region. The resulting upscaling capabilities could become beneficial for regional models.

3.2 Assimilation of HFR data

Hundreds of HF radar systems have been installed worldwide in both operational and experimental modes (Harlan et al. 2010; Willis, 2012). With their large area coverage, high resolution in time and space, and long-term operational capabilities, they enhanced the coastal ocean monitoring capabilities for surface currents (Paduan and Rosenfeld, 1996) and enabled developing new data products. The value of HF radar data for the investigation of circulation in the German Bight was demonstrated by Carbajal and Pohlmann (2004) and Port et al. (2011).

The present study addresses observations, numerical modelling, and a method proposed to carry out the blending of models and HF radar observations in an efficient and dynamically consistent way. Assimilation of HF radar data is not a trivial task because of irregular data gaps in time and space, inhomogeneous observation errors, and inconsistency between boundary

forcing and observations (Breivik and Saetra, 2001). The method developed by Stanev et al. (2015) and applied to the German Bight uses a spatiotemporal optimal interpolation (STOI) filter to improve short-term hindcasts and forecasts of surface currents. In the proposed approach, model simulations from a free run and radar observations acquired over periods of at least one tidal cycle were blended using the Kalman analysis equation. The focus on intra-tidal time scales and the data

5   assimilation technique used here explain the major differences from some earlier studies using 1) filtered data and 2) the classical Kalman analysis method, where observations and numerical simulations are usually combined at individual time steps. The proposed data assimilation approach has similarities with the methods described in Barth et al. (2010) and Sakov et al. (2010). However, it uses a simpler formulation of the model error covariance matrix, but at the same time addresses the forecast capability. The details of the approach are described in Stanev et al. (2015).

10

The method is able to provide short term forecasts for surface currents and was implemented as part of the pre-operational COSYNA system. The respective output is freely available on www.cosyna.de. An example of an analyzed current field together with the free model run and the HF radar measurements is shown in Fig. 4. The plot shows an outflow situation on March 22, 2011 at 17:00 UTC with current speeds exceeding 1 m/s in some areas. The high variability of currents is mostly

15   due to the combination between the strong tidal forcing and specific bathymetric features in the very shallow area. The green arrows represent the HF radar measurement, the blue arrows are the free model run and the red arrows are the analysis. Stanev et al. (2015) demonstrated that the analysis is in fact successful in improving the agreement of the model with the radar observations. It has been also shown that an improvement can furthermore be achieved with regard to independent ADCP data acquired outside the HF radar covered area, i.e., the analysis scheme has upscaling capabilities. The analysis

20   scheme can be run both in hindast and forecast mode. It will be shown in Sect. 4.2 that the proposed method, which is able to improve short term forecasts, is of practical relevance, e.g., for SAR.

3.3 Assimilation of temperature and salinity data

SST is one of the fundamental parameters determining water, heat and momentum exchange with the atmosphere, making these data a valuable observation for assimilation in ocean modelling. SST data are among the ones which are available from

25   both *in-situ* and remote sensing techniques and can be derived in the German Bight as comprehensive surface temperature analysis from remote sensing and as point observations from stationary and mobile platforms. One example for mobile platforms is the Ferry Box system. The latter is an autonomous measurement, data logging and transmission system, in which temperature and salinity measurements from samples of a continuous flow of seawater are taken from a water depth of 4-6 m while the carrying ship is on its way (Petersen et al., 2007).

30

As shown by (Grayek et al., 2011) the Ferry Box data have the capability to enhance the SST hindcast in the German Bight at least around the Ferry Box track. Using remote sensing analysis data from the Operational Sea Surface Temperature and

Sea Ice Analysis (OSTIA, Donlon et al., 2012) presents one alternative to using Ferry Box data. The advantage of the OSTIA data is its spatial coverage, however due to the applied processing procedures the data is smoother than other SST products (Donlon et al., 2012). In order to provide an optimal analysis with sufficiently high resolution a SST assimilation routine is used which handles all possible temporal/spatial combinations of the above mention data sources, allowing at the same time to include or exclude part of the observations. As seen in Fig. 5a, the yearly averaged RMSD between the free run for the nested German Bight model based on GETM (see Annex 6.2 and Staneva et al. (2009) describing the model) and OSTIA data does not exceed 0.5°C over large part of the German Bight. The errors in the Wadden Sea are attributed to the coarse resolution there (1 km), as well as to the possible problems with the relatively coarse OSTIA data. As it can be expected this error is strongly reduced if OSTIA data are assimilated (Fig. 5b).

The assimilation of OSTIA data complemented by SST and SSS observations form the Ferry Box system additionally improves the skill of the model (Fig. 6). The added value of using Ferry box data for data assimilation is clearly seen in the time series of surface temperature during 2011 (Fig.6a) and especially those of surface salinity (Fig.6b), when compared with the observations from the MARNET Ems Station.

The L3 multi-sensor super-collated SST product (CMEMS 2015) provides a higher spatial resolution and more information on smaller scales, but its temporal/spatial coverage depends on the satellite's revisit time and the cloud conditions. Another analysis is presented in Fig. 6c, which additionally assimilates these finer-resolution data, named 'DA BLEND'. The comparison between the experiments assimilating OSTIA data only and the 'DA BLEND' data reveals that the latter improves the representation of the short-term variability, which is associated with the synoptic-scale features. These features are not captured by the relatively smooth OSTIA data. However, without continuously using these additional observations (because of the missing data) their imprint in the model solution persists (in the strongly tidally driven coastal ocean) only for a couple of days. Afterwards the model returns to the state characteristic for the 'DA OSTIA' run, like it is, e.g., the case in the end of the analyzed period (after October 16th, 2011). Using observations from some existing fixed platforms (e. g., platforms-of-opportunities like offshore wind farms) could be beneficial for the future enhancement of the COSYNA pre-operational system.

4 German Bight applications

4.1 The usefulness of coastal forecasting

Maritime safety, management of marine resources, protecting coastal and marine environment, forecasting coastal weather, monitoring and seasonal and longer-term forecasting of coastal climate requires the integration of existing and newly emerging technologies with the aim to provide the society with the best estimates, including the quantitative information of errors. The methodology used today for merging, filtering and interpolating observations, most of which based on statistical

interpolation methods, needs further development in order to enable an adequate use of data from future observing systems. Of particular interest is to develop methods capable to make the best use of heterogeneous (in terms of space-time sampling and resolution) data. The deployment of new remote sensing and in situ observing systems could largely profit from both advancement in numerical modelling and data assimilation.

5

In the following part we will give several examples of useful application of coastal forecasting. The first one will demonstrate a possible enhancement of predictive capabilities for search and rescue operations by assimilating data from HF radars. The second example is on the estuarine applications. The third will demonstrate the usefulness of numerical modelling for assessing the possible impacts of wind parks on the coastal environment. The next one aims to give a

10 theoretical framework for understanding the problems arising from no-seamless modelling and understand that upscaling and downscaling cannot be treated/applied fully separately. The last example will be on the improvement of the forecasting skill for extreme events by using coupled circulation-wind wave models.

4.2 Particle tracking: Enhancement of SAR by HFR observations

The validation of data assimilation of HF radar data Stanev et al. (2015) demonstrated that HF-radar data can be not only

15 interpolated, but also 'extended' in space, which allows to generate homogeneous mapped data series. The key difference of the STOI method to other techniques, which provide extrapolated surface current fields based on HF radar data alone is that the STOI state estimates are dynamically consistent with a numerical model run. This is an important aspect when considering the use of such methods in operational systems, many of which have numerical models as their core part.

20 The following two experiments have been carried out using as an input the model data described in Sect. 3.2 (see also Fig. 5). In total 33746 Lagrangean particles (this number equals the number of wet model points) have been released every day starting from 00:00 on September 1, 2011 at the surface in the center of every grid cell and were 2-D tracked with a Lagrangean model. Trajectories were computed over three days using hourly model output from either analysis or free model run. The trajectory simulations for the same initial positions of particles have been restarted every day for the same

25 integration time of three days. The Lagrangean model output consisted of 33746x30x24 individual positions. In Fig. 7a the monthly averaged distance between positions of particles in the two runs 24 hours after the release is shown. Release locations from where particles reached the model boundary were excluded from the statistical analysis.

This map gives an idea about the expected success of SAR if data from HF radar are used or not used. In the latter case the

30 positioning of a lost object would be 3-6 km wrong after one day. Errors could be particularly big if the release is in the proximity of barrier islands or close to the northern model boundary. The complicated mesoscale currents around the Helgoland Island could pose problems in the model and observations and explain larger spatial variability of the error pattern. The trajectories from the two runs in 6 exemplary locations during three days of integration starting on September 5,

which are also shown on the same figure give an idea about the dominating propagation patterns, as well as an illustration that the coherence of tidal oscillations is lost relatively soon after the release. This illustrates the need for intra-tidal information from measurements to correct model trajectories.

5   The temporal evolution of the distance between particles released at the same positions (Fig. 7b) demonstrates the rapid increase of the distances between trajectories in the two runs. The averaged positioning error plotted by the dashed line gives an overall idea about accuracy in the search and rescue operations using output from the free run. The reduction of the error of positioning of an object due to the use of HF radar data during three days is about 10 km on average. It is obvious that using the HF radar data could provide a useful enhancement of the quality of surface currents' products in SAR applications.

4.3 Estuarine applications

Estuaries have been regions of intense human development from prehistoric times to the industrial age (Lotze et al., 2006). In modern times they have been increasingly shaped by human intervention, e.g., by the construction of harbours, construction of storm surge barriers and channel dredging (Talke et al., 2009; Schuttelaars et al., 2013). That is why today they are in the focus of the stakeholders' interest; sometimes these interests are divergent or conflicting. Increasingly the society seeks support from science in order to manage the estuarine and coastal space.

There is also a profound interest in the physical oceanography of estuaries. They constitute the border between the deep-ocean and land, and between salt water and freshwater (Dyer, 1973). They are subject to vigorous tidal currents and highly variable water level, featuring a great number of physical processes that interact to generate complex dynamics. Therefore coasts and estuaries present also a challenging research case for environmental studies and applications. One region of great interest to science and society is the Ems Estuary (see, e.g., Chernetsky et al., 2010). Being shaped to a great degree by storm surges during the Middle Ages, it is today entirely surrounded by dikes and its river part is protected by a storm surge barrier. Intense economic exploitation, especially regular dredging of the navigation channel, led to very high concentrations of suspended sediment in the tidal river (de Jonge et al., 2014).

So far the numerical modelling of realistic estuaries (with realistic topography, coasts, surface and open-boundary forcing, river runoff forcing, as well as adequately resolved baroclinicity and 3D turbulence) does not find a wide use in the estuarine forecasting practices. Unstructured numerical models are able to represent the multiple scales of coastal and estuarine dynamics, allowing for the study of subtidal, tidal and intermittent processes (Zhang and Baptista, 2008; Zhang et al., 2016, see also Annex 6.4). The model of the Ems Estuary developed by Pein et al. (2014) can be considered as a tool to tackle a number of research and practical questions regarding the functioning and the physical peculiarities of this specific region. In

the following we will illustrate the performance of this model in assessing the tidal distortion, which is fundamental for the sediment dynamics and its dependence on man-induced changes in this estuary.

The dominant dynamics in the Ems Estuary are induced by tides (van de Kreeke and Robaczewska, 1993). As demonstrated by Pein et al. (2014), who performed a series of numerical experiments with the SCHISM (see Annex 6.4) the M-2 amplitude (Fig. 8a - left panel) is small near the western open boundary of the model area and rises up to almost 1 m at the easternmost barrier island. In the Ems Estuary it clearly increases with the convergence of the topography, i.e., towards the tidal river and towards the eastern part of the back barrier region. Reaching a maximum of approximately 1.5 m at the entrance of the tidal river, the main lunar tide is damped near the head of the estuary (Fig. 8a).

The M-4 tide generally has a smaller amplitude (Fig. 8a - middle panel, see also Sect. 2.2.4). Its amplitude increases continuously towards the tidal weir. The ratio between M-4 and M-2 tidal amplitudes equals about 0.1 in the western part of the open sea and the outer estuary (Fig. 8a - right panel). In the eastern part of the open sea it has a minimum, which means that in this area the M-2 tide is almost not distorted by the M-4 tide. In the tidal river the M-4-to-M-2 ratio reaches 0.3 (the right most panel in Fig. 8a), indicating a strong distortion of the tidal wave. Near the tidal weir the M-4 tide apparently resonates with the local basin and attains half the amplitude of M-2 tide.

In the main estuarine channel the M-2 tide amplitude of the surface current grows continuously until km 77 from the tidal inlet (Fig. 8b). The maximum flood currents are much stronger than the ebb currents in most of the channel (Fig. 8b). Such a flood-ebb asymmetry is also revealed by the along-channel profile of the ratio of eddy viscosity during flood and ebb (Fig. 8c), which is the well-known tidal mixing asymmetry. The local minima of the current asymmetry around km 35 and km 57 coincide with the minima of the mixing asymmetry. The opposite is true for the flood currents and mixing around km 50. These asymmetries demonstrate the strong relationship between the tidal currents and tidal mixing.

The above examples highlight the abilities of the Ems Estuary model to capture the key processes of the estuarine dynamics (see, e.g., Geyer and MacCready, 2014) in this specific marine environment. Based on these results one could ask the questions: (1) how predictable is the dynamics in the Ems Estuary, (2) can the predictability be enhanced by using observations? As seen in Fig. 8a, the M2 and M4 tides reveal clear horizontal patterns, which are consistent with observations as shown in Pein et al. (2014). One can thus expect that, provided open-ocean forcing for the area is well known, tidal predictions could be used to infer the temporal-spatial changes in the estuary. This cannot be done for the entire area by using point-wise observations alone. One initial step was proposed by Pein et al. (2016), who investigated how well the estuarine state (e.g., salinity) could be reconstructed using a limited amount of synthetic (provided by the model) observations. A limited number of EOFs represents relatively accurately the total variability: EOF-1 and EOF-2 describe ~60 and ~20 percent of the total variability, respectively. The corresponding principle components reveal a clear M2 and M4

Ocean Science

Discussions

dominance (Fig. 9a). While the pattern of the EOF-1 follows the estuary and the tidal river (Fig. 9b), the one of EOF-2 (Fig. 9c) describes the major pathway of propagation of fresh water (ROFI). Since the amount of continuously available data, which could be used for statistical assimilation of observations is still very limited, statistical analyses, like the one presented by Pein et al. (2016), is very useful. One application is the identification of the dominant spatial and temporal characteristics

5   of estuarine dynamics and the errors of state estimates based upon the location and accuracy of observational platforms (Schulz-Stellenfleth and Stanev, 2010). The quantification of the representativeness of an observing network by including or excluding specific stations appears as a useful technique to assess the impact of an array of measuring devices (observational network design).

10   ## 4.4 The impact of wind parks on the coastal ocean: wakes behind constructions

The offshore wind energy industry in Europe is growing rapidly and at present already 69 wind farms in 11 countries have been installed, which extract a combined capacity greater than 6.5 GW (EWEA, 2013). This huge extraction of energy and offshore wind turbine constructions themselves could impact the protected coastal areas such as, e.g., the German Wadden Sea. Evidence from satellite images (Vanhellemont and Ruddick, 2014) show that wind park turbine piles can produce

15   wakes that are visible up to some hundreds of meters behind these constructions and influence the sediment distribution in the surrounding area.

To investigate this impact a setup using the ocean modelling system SCHISM (Zhang et al., 2016, see also Annex 6.4) was coupled with the sediment model of Pinto et al. (2012). The setup consists of a circular basin with a diameter of 10 km and a

20   depth of 21.6 m, which is in the range of typical depths around wind parks in the Southern German North Sea. The horizontal resolution in a circular zone around the piles with a diameter of 50 m is 1.5 m, decreasing to 5m in a circular zone of 7 km diameter and 100 m at the outer boundary which results in 4554487 triangular elements and 2277401 nodes. In the vertical direction 10 equidistant σ-layers are used (Grashorn and Stanev, paper submitted to Ocean Dynamics). The time step is 5 s and the simulations are performed in a barotropic mode. The conic-shaped piles are positioned in a rectangular pattern

25   with a side length of 800 m around the center of the model domain and are represented as bathymetric obstacles. At the open boundary the surface elevation is prescribed to mimic an anti-clockwise rotating M2 tide as

$$\zeta(x_b, y_b, t) = A \cdot (x_b \times \cos(\omega \cdot t) + y_b \cdot \sin(\omega \cdot t))$$

where $A = 10^{-5}$, x_b and y_b are the coordinates of the outer boundary, $\omega = 1.406257 \times 10^{-4}$ 1/s corresponds to the M2 frequency and t is the time. The resulting current speeds reach a maximum of ~0.7 m/s. The whole model setup can be interpreted as a

30   simplified part of a wind park in a coastal area in the Southern North Sea, where the eccentricity of tidal ellipses can be small. A sediment class is defined with the parameters shown in Table 1.

The simulated sediment wake at the water surface (Fig. 10) demonstrates that the concentration of SPM is very high close to the pile, where a maximum of turbulent kinetic energy can also be observed. The SPM is trapped in areas where Kármán vortices develop. The interaction of the wakes disturbs the pattern, but to first order it can be considered as a sum of the two independent individual wakes. The latter show a bending behavior, which can also be observed on the satellite images

5 (Vanhellemont and Ruddick, 2014). This wake generation and mobilization of SPM could lead to a net redistribution of sediments in the surrounding area of wind parks and have an environmental impact on coastal areas.

4.5 The concept of upscaling

There is an increasing number of coastal observatories becoming operational worldwide (Riethmüller et al., 2009; Stanev et al., 2011; Howarth and Palmer, 2011). This development is in particular driven by the growing need for information on

10 coastal processes relevant for the planning and management of human activities like, e.g., offshore wind farming. At the same time, big efforts are made in different parts of the world to setup operational models for the regional scale. For example, in Europe these activities are now organized in the framework of the Copernicus marine service (http://www.copernicus.eu/), which ensures that consistent regional model forecasts are provided for all European coastal areas.

15

Regional models, like the North West Shelf model used in the Copernicus marine service, are not able to resolve all relevant coastal processes. Downstream services for user groups interested in coastal information usually require higher spatial resolution. The usual approach to solve this problem is a nested setup, where a high resolution coastal model is coupled to a coarser model ("parent model") using either one-way or two-way coupling methods (Barth et al., 2005). Alternatively,

20 unstructured grid models are used to realize a seamless transition between different spatial scales (Zhang et al., 2015). Due to the high computational costs, the use of these models for operational applications is still limited up to now.

Also, the assimilation of observation data usually requires the use of high resolution models, because a lot of the small scale processes, e.g., monitored by HF radar systems, cannot be reproduced by regional scale models. To make best use of coastal

25 observations and to improve both coastal and regional scale forecasts, different aspects of nested model coupling require detailed analysis.

While the information propagation from coarser regional models to high resolution coastal models ("downscaling") is quite straightforward and well established, the information flow in the opposite direction ("upscaling") is quite demanding and

30 still subject of ongoing research. Different aspects of this problem are discussed in Schulz-Stellenfleth and Stanev (2016) for the barotropic dynamics in the North Sea. The two main aspects analyzed in this study were: 1) the impact of small scale information on the regional scale at the same location and 2) the impact of small scale information at one place on the regional scale at another place. The first point is of relevance, e.g., in the context of parameterization errors (e.g., bottom

roughness), while the second aspect is important for assimilation of coastal observations (in Sect. 2.3 this was illustrated when describing the coupling between the North Sea and Baltic Sea).

As shown in Schulz-Stellenfleth and Stanev (2016) observations acquired in the German Bight can in fact have a significant impact on the North Sea scale with the exact impact characteristics depending on the setup like, e.g., the open boundary conditions used for the North Sea model. The potential of coastal observations to improve the boundary forcing on a larger scale was also demonstrated in Barth et al. (2010). As an example Fig. 11 shows the water level standard deviation resulting from perturbations along the German Bight boundary.

4.6 Improving forecasting skill for extreme events

In the last decade the North European coasts were affected by severe storms, which caused serious damages in the North Sea coastal zones. Additionally, different human activities, e.g., offshore wind power industry, oil industry and coastal recreation necessitate information about the sea state in the coastal ocean with high resolution in space and time. There seems to be a consensus that high-quality predictions of extreme events, like storm surges and flooding caused by storms could contribute substantially to avoid or minimize human and material damages and losses. Therefore, reliable wave forecasts and long-term statistics of extreme wave conditions are of utmost importance for the coastal areas. In many coastal areas the need for reliable risk assessments also increases the demand for precise coastal predictions. This cannot be achieved without considering the wind wave-current interaction in coastal ocean operational forecasting. In this section we demonstrate the improvements of the forecasting skills during extreme events achieved by model coupling.

Oceanic flows can be strongly forced or modified by waves, in particular in the nearshore and in the coastal ocean (Lentz et al., 2008; Longuet-Higgins, 1970; Newberger and Allen, 2007). The interactions between surface waves and ocean currents control the boundary fluxes, momentum and energy exchange between the atmosphere and ocean, as well as important processes within the water column. Model coupling can be achieved at different levels of complexity. Rascle and Ardhuin (2009) demonstrated that a proper representation of the near-surface currents and drift requires the introduction of wave effects, in particular the Stokes drift and wave-induced mixing.

The German Bight is dominated by strong tidal currents therefore the nonlinear feedback between currents and waves plays an important role in this area. The coupling between the wave model (WAM) and the hydrodynamic model (GETM) improves the estimates of ocean state variables, especially in the coastal areas and estuaries (Staneva et al., 2015). The coupling in this study takes into consideration: (1) the effect of currents on waves and (2) the effects of waves on the upper ocean dynamics, in particular on mixing and drift currents.

The wave model WAM (The WAMDI group, 1988; Guenther et al. 1992) is used in COSYNA (and in the following analysis) to simulate the sea state in the southern North Sea. WAM is a 3rd generation non-stationary surface wave

prediction model based on the action density balance equation in frequency direction coordinates. Multiple nesting is possible. The model is forced by time series of surface (10 m) wind, wave spectra at open boundaries, currents and water level. The output from this model includes significant wave height, wave periods (Peak, Mean, Tm1, Tm2), wave direction, directional spread and wave spectra (frequency-direction). In WAM the thickness of water column and/or current fields can be non-stationary, grid points can fall dry and refraction due to spatially varying current is represented.

A representative example of the validation of the WAM in the German Bight is shown in Fig. 12 for the Elbe data station (see the position in Fig. 1) for the beginning of December 2013. Starting on the 5th of December the severe storm Xavier hit the coasts of Germany with westerly winds of above 30 m/s; the significant wave height was reaching up to ~8 m at the peak on the December, 6th, at 03 UTC.

The current wave model includes a revised approach for the wave breaking in coastal areas and a modified wave growth in the source term for the wind input. Neglecting the wave breaking which is very important in the shallow coastal area, results in a severe overestimation of the observed significant wave height at the peak of the storm (see the black curve in Fig. 12 with unrealistically high values). When the new improved option for the wave breaking is taken into account, the model results show much better agreement with the observations (orange curve). The best match between modelled and measured data is achieved finally with the additional use of the modified wave growth parametrization, which ensures a more appropriate adaption to the driving wind fields (blue curve). That is supported by the statistics generated for three buoys' locations in the German Bight, and as seen in Table 2, the statistical parameters are improved significantly using the new modified version of the COSYNA wave model.

The German Bight GETM set up (see Annex 6.3) was modified to account for the wave effects by introducing the depth dependent radiation stresses and Stokes drift. These terms were calculated from the integrated wave parameters according to Mellor (2008). The gradient of the radiation stress serves as an additional explicit wave forcing term in the momentum equations for the horizontal velocity components. The transfer of momentum by waves becomes important for the mean water level setup (Fig. 13a) and for the alongshore currents generated by waves in the surf zone.

We demonstrate the role of the wave-induced forcing on hydrodynamics by showing the horizontal patterns of the maximum difference between sea level in four coupled simulations (having different level of complexity) and the circulation model only. These differences are computed at each grid point during the period of an extreme event (storm "Xaver"), which appeared from 02.12.2013 to 10.12.2012. The patterns show that the simulated surge differences between the coupled and circulation only model are more pronounced along the coastal areas of the German Bight. The maximum difference is about 40 cm in the North Frisian Wadden Sea region (Fig.13a). In the open sea the differences in the simulated surge characteristics are negligible. The sea level variability for the Helgoland tide gauge (Fig. 13b) demonstrates that during normal meteorological conditions the coupled and non-coupled models fit well with the tide gauge data. However, during the

storm Xavier, the sea level predicted by the pure hydrodynamic model is underestimated by more than 30 cm. It appears that the sea level predictions of the coupled model are closer to the tide gauge measurements (compare the green symbols and black lines).

The basic conclusion from this part is that the large differences between numerical simulations in coupled and un-coupled
5   modes indicates that accounting for the wind-wave effects in the three dimensional hydrodynamic model improves predictions of water level in the shallow coastal waters. Predictions of storm events with coupled models could be of utmost importance for many coastal applications dealing with risk analyses (e.g., off-shore wind industry, oil platform operations, etc.), where higher accuracy is needed. This justifies the consideration of waves in the operational forecasting.

5 Conclusions

10   One of the aims of the present study was to present some developments contributing to coastal ocean forecasting with a focus on new modelling issues, coupling between models, data assimilation and research towards practical applications. The large number of issues and the fact that some previous publications already exist on the individual research question led us to the decision to present here a review on the modelling-related COSYNA activities, some of which have been already implemented in the COSYNA pre-operational suite. In order to keep the volume of this paper in a reasonable limit we just
15   showcase methodologies and new developments, referring to more extended original publications, if available.

In the heart of the North Sea dynamics is the tidal forcing, to which much consideration has been given in the past. However, so far not enough inter-comparison studies exist on the performance of individual models to adequately simulate tides, and in particular the shallow-water tides. These shallow-water tides are very important for the tidal dynamics in the coastal areas,
20   where the tidal range is larger than in the open-ocean, and the propagation of tidal waves is more complex. One manifestation of this complexity is the non-linear physics, which many models do not well simulate. This is exemplified by the comparison between simulated shallow-water tides in the individual models. We compared the tide analyses from six models, which were set up for almost the same ocean area and demonstrated that the M4-tide amplitudes show pronounced differences in all models. Unlike the good agreement in the M2 phases, the phases of shallow-water tides differ substantially.
25   This is just one demonstration about how different the representation of the non-linearity in the analyzed *regional* models is. With the exception of SCHISM, all other considered models were using resolutions of several kilometers, which is not sufficient to resolve shallow-water tides. This could be one of the candidates to explain the differences in the simulated non-linear tidal dynamics, and in particular the distortion of tidal signals in the shallow coastal zone of the North Sea.

30   In all models M4 tides have smaller spatial scales compared to the M2 tides. Although they also have very small magnitudes they are very important for the asymmetric in time tidal dynamics of coastal ocean and the resulting net transport of mater.

Therefore, further attention is needed with respect to their adequate representation in the numerical regional and coastal models.

The model inter-comparison demonstrated that the closed boundary in the Danish Straits in the FOAM-AMM7, which is operated only for the North-west shelf, results in a generation of an amphidromic point in the Kattegat, which was not observed in all other models (coupled with the Baltic Sea). This demonstrates how important is to have the North and Baltic Sea models coupled. However, this issue can easily be solved, as shown by most of model simulations described here. More fundamental is that it is still unknown what the optimal nesting is, which has to be applied to the transition area between the North Sea and Baltic Sea. We demonstrated some first results on the performance of a new two-way nesting method enabling the usage of different vertical discretization in the individual nests of the North Sea-Baltic Sea NEMO using regionally-appropriate vertical resolution (σ-coordinates in the shallow and tidally dominated North Sea and z-coordinates in the strongly stratified Baltic Sea) in order to avoid problems with the adequacy of the applications to different ocean areas (in the illustrated case the shallow and well mixed North Sea and the strongly stratified Baltic Sea). The presented method allows to up-scale the information from the fine resolution nest onto the coarser resolution simulation maintaining at the same time the overall dynamical consistency. We demonstrated that the fine-resolution nesting enhances the long-channel changes of stratification, which can be explained by the more realistic simulation of the secondary (transversal) circulation.

With respect to the coupling between different models in the narrow straits the application of unstructured-grid models seems an unavoidable research path. We did not consider here this issue for the Baltic Sea straits, although the numerical simulations with SCHISM were included in the inter-comparison Sect. 2.2. This is because this issue was addressed in detail by Zhang et al. (2016) and we decided to illustrate here another two different applications of unstructured-grid modelling. Using SCHISM as a tool to tackle the estuarine dynamics, we addressed the representation of tidal asymmetry in the Ems Estuary. It was shown that the ratio between amplitudes of M4 and M2 tide reaches 0.3 indicating a strong distortion of the tidal wave. The transport resulting from this tidal asymmetry could affect the accumulation of sediment.

In the second application of unstructured-grid modelling we presented results from numerical simulations of dynamics in and around a simplified wind park in the coastal area of the Southern North Sea. The model has extremely fine horizontal resolution of about 1m and was coupled with a suspended sediment model. The numerical simulations were analyzed in order to investigate the impact of wind parks on the dynamics in the area of wind parks. For the studied scales of about 1 km the model enabled simulation of Karman vortices and turbulent wakes. The simulated bending of the sediment plumes replicated very well the wakes observed on the satellite images (Vanhellemont and Ruddick, 2014). This wake generation and mobilization of SPM could lead to a net redistribution of sediments in the surrounding area of wind parks and have an environmental impact on coastal areas.

Ocean Science
Discussions

Open Access

EGU

COSYNA makes available large amount of data from different platforms and sensors. Among these, the HF radar data, with their large area coverage, high resolution in time and space, and long-term operational capabilities, could become a valuable data source for monitoring surface currents and other operational activities. We demonstrated the contribution of the developed spatio-temporal optimal interpolation (STOI) filter to improve short-term hindcasts and forecasts of surface

5   currents using observations from three continuously operating radars in the German Bight. The method is able to provide short term forecasts for surface currents and was implemented as part of the pre-operational COSYNA system. Its application demonstrated that the analysis provides continuous and homogenous data series over the entire German Bight and is successful to improving the agreement of the model with the radar observations. One application of the STOI in improving the quality of the Lagrangean particle tracking showed that the reduction of the error of positioning of an object

10   due to the use of HF radar data during three days is about 10 km on average, which makes clear that the HF radar data can be used to enhance SAR.

With respect to the assimilation of temperature and salinity data it has been shown that OSTIA data does not substantially improve the quality of predictions in the Wadden Sea. This is attributed to the coarse resolution there (1 km model resolution

15   was used), as well as to the possible problems with the relatively coarse-resolution data which were assimilated. The use of observations from the Ferry Box system additionally improves the skill of the model. The assimilation of SST data with a very high spatial resolution performs very accurately improving largely the representation of the synoptic-scale features. However, the temporal and spatial coverage of these data depend on the satellite's revisit time and the cloud conditions. The experiments performed demonstrated that without a frequent use of these observations (because of the missing data) their

20   imprint in the model solution persists only for a couple of days because the "memory" of the shallow-water physical system is short.

Another issue, which is very relevant to the regional ocean forecasting, is that models are not able to resolve all relevant coastal processes. The propagation of information from coarser regional models to high resolution coastal models

25   ("downscaling") is quite straightforward and well established therefore even the one-way nesting can sometimes provide good results. However, the information flow in the opposite direction ("upscaling") is quite demanding and still subject of ongoing research. We gave one illustration of the impact of small scale information at coastal scales on the regional-scale motion. This elucidated the potential of coastal observations to improve the boundary forcing on a larger scale, which is crucial when coupling between coastal and regional forecasting systems is concerned.

30

The improvement of the quality of predictions of wind waves in the coastal ocean has a large practical value. This improvement is strongly depending on the model physics, which is very sensitive to shallow depths. We demonstrated that the large differences between numerical simulations in coupled and un-coupled models indicate that accounting for the wind-wave effects in the three dimensional hydrodynamic model improves predictions in the shallow coastal waters. The

presented illustrations from coupled and un-coupled wave and circulation models made clear that large part of the uncertainties result from the nonlinear feedback between strong tidal currents and wind-waves. This can no longer be ignored in the theoretical studies and operational applications, in particular in the coastal zone, where its role seems to be dominant. Thus, precise coastal predictions cannot further neglect the wind wave-current interaction in the coastal ocean. In
5   particular, predictions of storm events with coupled models could be of utmost importance for many coastal applications dealing with risk analyses (e.g., off-shore wind industry, oil platform operations, etc.), where higher accuracy is needed.

Finally we want to remind that some of the examples considered here are relevant to the service evolution strategy of the Copernicus Marine Environment Marine Service (CMEMS, see also http://copernicus.eu/) and can be considered as a
10   research input to the operational oceanography. The relevant document, which is prepared by the CMEMS Scientific and Technical Advisory Committee (STAC), available at
 (https://www.mercator-ocean.fr/wp-content/uploads/2015/11/13-CMEMS-Service_evolution_strategy_RD_priorities.pdf)
has largely motivated us to put together the results of our recent research.

6 Annexes

15   ### 6.1 NEMO

The primitive equation ocean model NEMO (Nucleus for European Modelling of the Ocean) is a flexible tool for studying the ocean over a wide range of space and time scales (Madec, 2008). In the inter-comparison study considered in Sect. 2 model data from two NEMO setups are used. The first data set is from the Copernicus Marine environment monitoring service (http://marine.copernicus.eu) for the north-west shelf. The output is provided by the Forecasting Ocean Assimilation
20   Model- Atlantic Margin model with 7km resolution (FOAM-AMM7, O'Dea et al. 2012). The model uses 32 terrain following sigma-levels in the vertical.

The second setup is a development for the North Sea – Baltic Sea at the Helmholtz-Zentrum Geesthacht (NEMO-HZG; Grayek and Stanev, paper in preparation). The model area for the second setup extends from -4°9′Ex48°29′N to
25   30°11′Ex65°54′N. In its standard version the model uses a 2 nm resolution in the horizontal and 21 sigma-levels in the vertical. The model area is shown in Fig 2.

The air-sea fluxes are estimated using bulk formulas and 6-hourly atmospheric forcing fields derived from the ERA-Interim hindcast data-set, which is produced by the European Center for Medium-Range Weather Forecasts (ECMWF). At the open
30   lateral boundaries the model is forced with 4D interpolated temperature and salinity profiles calculated from the monthly climatological data of Janssen et al. (1999). The boundary conditions for currents and sea surface elevation at the lateral

boundaries are derived from harmonic tidal analyzes provided by the Oregon State University Tidal Inversion Software (OTIS). Water fluxes at the surface include ERA-Interim precipitation.

6.2 GETM

GETM (General Estuarine Transport Model) is a primitive equation prognostic three-dimensional hydrodynamic model. The use of generalized vertical coordinates makes it suitable for shallow coastal regions under the influence of tidal currents (Burchard and Bolding, 2002). In this model the equations for the three velocity components, sea-surface height, temperature, salinity, as well as the equations for turbulent kinetic energy and the eddy dissipation rate due to viscosity are solved. A particular feature of GETM is its ability to adequately represent the dynamics in deep inlets and channels as well as on the tidal flats, the latter falling dry during part of the tidal period (Stanev et al., 2003a).

The nested modelling system based on GETM consists of three model configurations: a coarse-resolution (about 5 km) North Sea-Baltic Sea outer model, a fine-resolution (about 0.8 km) inner model covering the German Bight and a very fine-resolution (about 200 m) model for the Wadden Sea region resolving the barrier islands and the tidal flats (for more detailed presentation of the model area and set up, see Staneva et al., 2009). The bathymetric data for the different model configurations are prepared using the ETOPO-1 topography, together with observations made available from the BSH. The model system is forced by: (1) atmospheric fluxes estimated by the bulk formulation using 1-hourly forecasts from the German Weather Service (DWD), (2) hourly river runoff data provided by the BSH operational model, and (3) time-varying boundary conditions of sea surface elevations and salinity. The sea surface elevations at the open boundary of the North Sea-Baltic Sea model are generated using tidal constituents obtained from the TOPEX/POSEIDON harmonic tide analysis. Temperature and salinity at the open boundary of the outer model are interpolated at each time step using the monthly mean climatological data of Janssen et al. (1999). The fresh-water fluxes from the main tributaries in the region are taken from the observations available from the Niedersächsischer Landesbetrieb für Wasserwirtschaft und Küstenschutz, Aurich, Germany.

6.3 BSHcmod

BSHcmod is a three dimensional prognostic model (Dick et al., 2001; Dick and Kleine, 2007), which was developed at the German Federal Maritime and Hydrographic Agency (BSH). The model is used for operational applications and is run in a two-way nested configuration providing information on sea-level, temperature, salinity and currents in the North Sea and the Baltic Sea. In the standard operational setup the model is used for 72 hrs forecasts. The model provides input to drift and dispersion models, which are operated on demand.

A version of the model described above with adaptive vertical coordinates (Dick and Kleine, 2007) was made available to the authors by the BSH and used to generate another output data set which is analyzed in the present study. A grid with 900 m resolution was used for the German Bight and a coarser resolution of 5 km was used for the remaining part of the North

Ocean Science
Discussions

Sea and the Baltic Sea. The open boundary conditions are formulated using sea level data calculated from the tidal constituents of 14 partial tides. Data from the German Weather Service (DWD) were used for the wind forcing and climatological data were used for river discharge. The code was run on 8 processors using the OpenMP library. The data analysis is based on model results for the year 2011. The 5 km model grid is identical to the one of the operational model

5   described above (see Fig. 2).

6.4 SCHISM

Unstructured-grid models enable a seamless transition between processes at coastal and open-ocean scales. SCHISM (Semi-implicit Cross-scale Hydroscience Integrated System Model; Zhang et al., submitted), which is a successor of the original model of Zhang and Baptista (2008) is one such model. New developments since the last writing (Zhang et al. 2015) include

10   addition of mixed triangle-quadrangles grid, and 1D/2D/3D options all wrapped in a single model grid. SCHISM solves the hydrostatic Reynolds-averaged Navier–Stokes equations with transport of heat, salt and tracers in the hydrostatic form with Boussinesq approximation on unstructured grids. The efficiency and robustness of SCHISM are mostly attributed to the implicit treatment of all terms that place stringent stability constraints (e.g., CFL) and the use of Eulerian-Lagrangian method for the momentum advection. The vertical grid allows using partially terrain-following S-and partial Z-coordinates (flexible

15   localized sigma coordinates with shaved cell, Zhang et al., 2015).

The set-up of SCISM for the North Sea-Baltic Sea area is described by Zhang et al. (2016); the model area is shown in Fig. 2 Altogether there are ~300K nodes and ~600K triangles, with refinement along the German Bight and Danish straits, where a nominal resolution of 200 m is used. On the open North Sea boundaries (Scottish Shelf and English Channel) time series of

20   elevation, horizontal velocity, salinity and temperature are interpolated from MyOcean products (http://www.myocean.eu).The sea–surface boundary conditions use the output from the regional model COSMO EU (wind, atmospheric pressure, air temperature and specific humidity) operated by the German Weather Service with a horizontal resolution of 7km. Heat fluxes (including solar radiation and downward long wave (infrared) radiation needed as surface boundary condition come from the NOAA's CFSR product (http://www.ncdc.noaa.gov/data-access/model-data/model-

25   datasets/climate-forecast-system-version2-cfsv2). Monthly flow data at 33 rivers in the region are provided by the BSH.

References

5 Andersen, O. B.: Shallow water tides in the northwest European shelf region from TOPEX/POSEIDON altimetry, J. Geophys. Res., 104, 7729–7741, doi:10.1029/1998JC900112, 1999.

Andersen, O. B., Egbert, G. D., Erofeeva, S. Y., and Ray, R. D.: Mapping nonlinear shallow-water tides: a look at the past and future, Ocean Dynam., 56, 416-429, 2006.

10

Barth, A., Alvera Azcarate, A., Gurgel, K. W., Staneva, J., Port, A., Beckers, J. M., and Stanev, E. V.: Ensemble perturbation smoother for optimizing tidal boundary conditions by assimilation of High-Frequency radar surface currents-application to the German Bight, Ocean Sci., 6, 161-178, 2010.

15 Breivik, O., and Saetra, O.: Real time assimilation of HF radar currents into a coastal ocean model, J. Marine Syst., 28, 161–182, 2001.

Burchard, H., and Bolding, K.: GETM: A General Estuarine Transport Model, Scientic Documentation, No EUR 20253 EN, European Commission, printed in Italy, 157, 2002.

20

Cailleau, S., Fedorenko, V., Barnier, B., Blayo, E., and Debreu, L.: Comparison of different numerical methods used to handle the open boundary of a regional ocean circulation model of the Bay of Biscay, Ocean Model., 25, 1–16, 2008.

Carbajal, N., and Pohlmann, T.: Comparison between measured and calculated tidal ellipses in the German Bight, Ocean
25 Dynam., 54, 520–530, 2004.

Chabert d'Hières, G., and Le Provost, C.: Determination des characteristiques des ondes harmoniques M2 et M4 dans la manche sur modele reduit hydraulique, CR Acad. Sci. Paris 270:1703–1706, 1970.

30 Chassignet, E., and Verron, J. (eds.): Ocean Weather Forecasting: An Integrated View of Oceanography, Springer, Netherlands, 2006. 578 pages.

Ocean Science
Discussions

Open Access

EGU

Chernetsky, A. S., Schuttelaars, H. M., and Talke, S. A.: The effect of tidal asymmetry and temporal settling lag on sediment trapping in tidal estuaries, Ocean Dynam., 60, 1219-1241, 2010.

5   CMEMS: Product User Manual for Level 3 SST products over European Seas, CMEMS-OSI-PUM-010-009(1.3), 38, url: http://marine.copernicus.eu/documents/PUM/CMEMS-OSI-PUM-010-009.pdf, 2015.

Cummings, J. A., Bertino, L., Brasseur, P., Fukumori, I., Kamachi, M., Martin, M. J., … and Weaver, A. : Description of assimilation methods used in GODAE systems, Oceanography Magazine, 22, 96-109, 2009.

10

de Jonge, V. N., Schuttelaars, H. M., van Beusekom, J. E., Talke, S. A., and de Swart, H. E.: The influence of channel deepening on estuarine turbidity levels and dynamics, as exemplified by the Ems estuary, Estuar. Coast. Shelf S., 139, 46-59, 2014.

15   De Mey, P., Craig, P., Davidson, F., Edwards, C. A., Ishikawa, Y., Kindle, J. C., ... and Zhu, J.: Applications in coastal modeling and forecasting, Oceanography, *22*, 198-205, 2009.

De Mey, P., and Proctor, R.: Assessing the value of GODAE products in coastal and shelf seas, Ocean Dynam., *59*, 1-2, 2009.

20

Dick, S., and Kleine, E.: The BSH New Operational Circulation Model Using General Vertical Coordinates, Environmental Research, Engineering and Management, 3, 18-24, 2007.

Dick, S.K., Kleine, E., Muller-Navarra, K.., Klein, S.H., and Komo, H.: The operational circulation model of BSH
25   (BSHcmod): Model description and validation, Berichte des Bundesamtes fuer Seeschifffahrt und Hydrographie (BSH), 29, 49, 2001.

Donlon, C.J., Martin, M., Stark, J., Roberts-Jones, J., Fiedler, E., and Wimmer, W.: The operational sea surface temperature and sea ice analysis (ostia) system, Remote Sens. Environ., 116, 140-158, doi:10.1016/j.rse.2010.10.017, 2012.

30

Döös, K., Meier, H. E. M., and Döscher, R.: The Baltic haline conveyor belt or the overturning circulation and mixing in the Baltic, AMBIO: A Journal of the Human Environment, 33, 261-266, 2004.

Dyer, K. R.: Estuaries: A physical introduction, John Wiley, 1973.

Egbert, G. D., Erofeeva, S. Y., and Ray, R. D.: Assimilation of altimetry data for nonlinear shallow-water tides: Quarter-
5   diurnal tides of the Northwest European Shelf, Cont. Shelf Res., 30, 668-679, 2010.

European Wind Energy Association (EWEA): The European offshore wind industry-key trends and statistics 2013, url:
http://www.ewea.org/fileadmin/files/library/publications/statistics/European_offshore_statistics_2013.pdf , 2014.

10 Feistel, R., Nausch, G., Hagen, E.: Unusual baltic inflow activity in 2002-2003 and varying deepwater properties,
Oceanologia, 48, 2006.

Flather, R. A.: A tidal model of the northwest European continental shelf, Mem. Soc. R. Sci. Liege, 10,141-164, 1976.

15 Flather, R. A.: Results from a model of the north-east Atlantic relating to the Norwegian Coastal Current, The Norwegian
Coastal Current, eds. R. Sætre and M. Mork, University of Bergen, 2, 458, 1981.

Geyer, W. R., and MacCready, P.: The estuarine circulation, Annu. Rev. Fluid Mech., 46.1 , 175, 2014.

20 Golbeck, I., Li, X., Janssen, F., Brüning, T., Nielsen, J. W., Huess, V., ... and Hackett, B.: Uncertainty estimation for
operational ocean forecast products—a multi-model ensemble for the North Sea and the Baltic Sea, Ocean Dynam., 65,
1603-1631, 2015.

Grayek, S., Staneva, J., Schulz-Stellenfleth, J., Petersen, W., and Stanev, E. V.: Use of FerryBox surface temperature and
salinity measurements to improve model based state estimates for the German Bight, J. Marine Syst., 88, 45-59, 2011.

25 Guenther, H., Hasselmann, S., and Janssen, P.A.E.M.: The WAM Model User Manual, Deutsches Klimarechenzentrum,
Technical Report, 1992.

Harlan, J., Terrill, E., Hazard, L., Keen, C., Barrick, D., Whelan, C., ... and Kohut, J. : The Integrated Ocean Observing
System high-frequency radar network: Status and local, regional, and national applications, Mar. Technol. Soc. J., 44, 122-
30 132, 2010.

Jacob, B., Stanev, E. V., and Zhang, Y.J.: Local and Remote Response of the North Sea Dynamics to Morphodynamic Changes in the Wadden Sea, Ocean Dynam., 66, 5, 671-690, 2016.

Jouanno, J., Sheinbaum, J., Barnier, B., Molines, J. M., Debreu, L., and Lemarié, F.: The mesoscale variability in the
5   Caribbean Sea. Part I: Simulations and characteristics with an embedded model, Ocean Model., 23, 82-101, 2008.

Korres, G., Triantafyllou, G., Petihakis, G., Raitsos, D.E., Hoteit, I, Pollani, A.: A data assimilation tool for the Pagasitikos Gulf ecosystem dynamics: Methods and benefits, Journal of Marine Systems 94, 102-117, 2012.

10 Kourafalou, V. H., De Mey, P., Le Hénaff, M., Charria, G., Edwards, C. A., He, R., ... and Usui, N.: Coastal Ocean Forecasting: system integration and evaluation, Journal of Operational Oceanography, 8, 127-146, 2015.

Kourafalou, V. H., De Mey, P., Staneva, J., Ayoub, N., Barth, A., Chao, Y., ... and Moore, A. M.: Coastal Ocean Forecasting: science foundation and user benefits. Journal of Operational Oceanography, 8, 147-167,
15 doi:10.1080/1755876X.2015.1022348, 2015.

Laurent, D., Eric, B., and Bernard, B.: A general adaptive multi-resolution approach to ocean modelling: Experiments in a primitive equation model of the North Atlantic, Lect. Notes Comp. Sci., 303-313, Springer, 2005.

20 Lindström, G., Pers, C., Rosberg, J., Strömqvist, J., and Arheimer, B.: Development and testing of the HYPE (Hydrological Predictions for the Environment) water quality model for different spatial scales, Hydrol. Res., 41, 295-319, 2010.

Longuet-Higgins M.S., and Stewart R.W.: Radiation stresses in water waves: a physical discussion with applications, Deep-Sea Res., 11, 529–562, 1964.

Lotze, H. K., Lenihan, H. S., Bourque, B. J., Bradbury, R. H., Cooke, R. G., Kay, M. C., ... and Jackson, J. B.: Depletion,
25 degradation, and recovery potential of estuaries and coastal seas, Science, 312, 1806-1809, 2006.

Madec, G.: NEMO ocean engine. Note du Pole de modelisation, 1 Institut Pierre-Simon 2 Laplace (IPSL), France, 27, ISSN 1288-1619, 217, 2008.

30 Malanotte-Rizzoli, P., Young, R. E., and Haidvogel, D. B.: Initialization and data assimilation experiments with a primitive equation model, Dynam. Atmos. Oceans, 13, 349-378, 1989.

Meier, H. E., and Kauker, F.: Modeling decadal variability of the Baltic Sea: 2. Role of freshwater inflow and large-scale atmospheric circulation for salinity, J. Geophys. Res., 108, C11, 2003.

Mellor, G.L.: The Depth-Dependent Current and Wave Interaction Equations: A Revision, J. Phys. Oceanogr., 38, 2587-2596, doi:10.1175/2008JPO3971.1, 2008.

Newberger, P. A., and J. S. Allen: Forcing a three-dimensional, hydro-static primitive-equation model for application in the surf zone: 1. Formulation, J. Geophys. Res., 112, C08018, doi:10.1029/2006JC003472, 2007.

O'dea, E. J., Arnold, A. K., Edwards, K. P., Furner, R., Hyder, P., Martin, M. J., ... and Liu, H.: An operational ocean forecast system incorporating NEMO and SST data assimilation for the tidally driven European North-West shelf, Journal of Operational Oceanography, 5, 3-17, 2012.

Paduan, J. D., and Rosenfeld, L. K.: Remotely sensed surface currents in Monterey Bay from shore-based HF radar (Coastal Ocean Dynamics Application Radar), J. Geophys. Res., 101, 20669–20686, 1996.

Pein, J. U., Grayek, S., Schulz-Stellenfleth, J. and Stanev, E. V.: On the impact of salinity observations on state estimates in Ems Estuary. Ocean Dynam., 66:243–262, 2016.

Pein, J. U., Stanev, E. V., and Zhang, Y. J.: The tidal asymmetries and residual flows in Ems Estuary, Ocean Dynam., 64, 1719-1741, 2014.

Petersen, W., Colijn, F., Hydes, D., and Schroeder, F.: Ferrybox: From on-line oceanographic observations to environmental information, Eurogoos publication, 25, SHMI, 2007.

Pinto, L., Fortunato, A.B., Zhang, Y., Oliveira, A., and Sancho, F.E.P.: Development and validation of a three-dimensional morphodynamic modelling system for non-cohesive sediments, Ocean Model., 57-58, 1-14, 2012.

Port, A., Gurgel, K. W., Staneva, J., Schulz-Stellenfleth, J., and Stanev, E. V.: Tidal and wind-driven surface currents in the German Bight: HFR observations versus model simulations, Ocean Dynam., 61, 1567-1585, 2011.

Proudman, J., and Doodson, A.T.: The principal constituent of the tides of the North Sea, Philos. T. R. Soc. Lond., 224, 185-219, 1924.

Ocean Science
Discussions

Open Access

EGU

Le Provost, C.: Generation of overtides and compound tides (review), Tidal Hydrodynamics, 269- 296, John Wiley, New York, 1991.

Rascle, N., and F. Ardhuin: Drift and mixing under the ocean surface revisited: Stratified conditions and model-data comparisons, J. Geophys. Res., 114, C02016, doi:10.1029/2007JC004466, 2009.

5   Riethmüller, R., Colijn, F., Krasemann, H., Schroeder, F., and Ziemer, F.: COSYNA, an integrated coastal observation system for Northern and Arctic Seas, OCEANS 2009-EUROPE, 1-7, IEEE, 2009.

Sakov, P., Evensen, G., and Bertino, L.: Asynchronous data assimilation with the EnKF, Tellus A, 62, 24-29, 2010.

10 Sayin, E., Krauß, W.: A numerical study of the water exchange through the Danish straits, Tellus 48, 324–341, 1996.

Schulz-Stellenfleth, J., and Stanev, E. V.: Statistical assessment of ocean observing networks: A study of water level measurements in the German Bight, Ocean Model., 33, 270–282, doi:10.1016/j.ocemod.2010.03.001, 2010.

15 Schulz-Stellenfleth, J., and Stanev, E. V.: Analysis of the upscaling problem - A case study for the barotropic dynamics in the North Sea and the German Bight, Ocean Model., in press, 2016.

Schuttelaars, H. M., de Jonge, V. N., and Chernetsky, A.: Improving the predictive power when modelling physical effects of human interventions in estuarine systems, Ocean Coast. Manage., 79, 70-82, 2013.

20

Siddorn, J. R., Good, S. A., Harris, C. M., Lewis, H. W., Maksymczuk, J., Martin, M. J., and Saulter, A.: Research priorities in support of ocean monitoring and forecasting at the Met Office, Ocean Science, 12(1), 217-231, doi:10.5194/os-12-217-2016, 2016.

25 She, J., Allen, I., Buch, E., Crise, A., Johannessen, J. A., Le Traon, P. Y., Lips, U., Nolan, G., Pinardi, N., Reißmann, J. H., Siddorn, J., Stanev, E., and Wehde, H.: Developing European operational oceanography for Blue Growth, climate change adaptation and mitigation and ecosystem-based management, Ocean Sci. Discuss., doi:10.5194/os-2015-103, in review, 2016.

30 She, J., Berg, P., Berg, J.: Bathymetry impacts on water exchange modelling through the Danish Straits, J. Marine Syst., 65, 450-459, 2007.

Shum, C. K., Woodworth, P. L., Andersen, O. B., Egbert, G. D., Francis, O., King, C., ... and Parke, M. E.: Accuracy assessment of recent ocean tide models, J. Geophys. Res., 102, 25173-25194, 1997.

Stanev, E. V., Schulz-Stellenfleth, J., Staneva, J., Grayek, S., Seemann, J., amd Petersen, W.: Coastal observing and forecasting system for the German Bight–estimates of hydrophysical states, Ocean Sci., 7, 569-583, 2011.

Stanev, E. V., Ziemer, F., Schulz-Stellenfleth, J., Seemann, J., Staneva, J., and Gurgel, K. W.: Blending Surface Currents from HF Radar Observations and Numerical Modeling: Tidal Hindcasts and Forecasts, J. Atmos. Ocean. Tech., 32(2), 256-281, 2015.

Staneva, J., Stanev, E. V., Wolff, J. O., Badewien, T. H., Reuter, R., Flemming, B., ... and Bolding, K.: Hydrodynamics and sediment dynamics in the German Bight. A focus on observations and numerical modelling in the East Frisian Wadden Sea, Cont. Shelf Res., 29, 302-319, 2009.

Staneva, J., Wahle, K., Günther, H., and Stanev E.V.: Coupling of wave and circulation models in coastal-ocean predicting systems: A case study for the German Bight, MS No.: OS-2015-86, Special Issue: Operational oceanography in Europe 2014 in support of blue and green growth, 12, 3169–3197, 2015.

Stips, A., Bolding, K., Pohlmann, T., and Burchard, H.: Simulating the temporal and spatial dynamics of the North Sea using the new model GETM (general estuarine transport model), Ocean Dynam., 54, 266-283, 2004.

Su, J., Sein, D. V., Mathis, M., Mayer, B., O'Driscoll, K., Chen, X., ... and Pohlmann, T.: Assessment of a zoomed global model for the North Sea by comparison with a conventional nested regional model, Tellus A, 66, doi:10.3402/tellusa.v66.23927, 2014.

Storch, H.v., Emeis, K., Meinke, I., Kannen, A., Matthias, V., Ratter, B. M., ... and Wirtz, K.: Making coastal research useful–cases from practice, Oceanologia, 57, 3-16, 2015.

Talagrand, O.: On the damping of high-frequency motions in four-dimensional assimilation of meteorological data, J. Atmos. Sci., 29, 1571-1574, 1972.

Vanhellemont, Q., and Ruddick, K.: Turbid wakes associated with offshore wind turbines observed with Landsat 8, Remote Sens. Environ., 145, 105–115, 2014.

Ocean Science
Discussions

Open Access

EGU

Talke, S. A., de Swart, H. E., and Schuttelaars, H. M.: Feedback between residual circulations and sediment distribution in highly turbid estuaries: an analytical model. Cont. Shelf Res., 29, 119-135, 2009.

Van de Kreeke, J., and Robaczewska, K.: Tide-induced residual transport of coarse sediment; application to the Ems estuary, Neth. J. Sea Res. , 31, 209-220, 1993.

Willis, Z.: Towards a global HF radar network, Journal of Operational Oceanography, *5*, 2-2, 2012.

Woodworth, P. L., and Thomas, J.P.: Determination of the major semidiurnal tides of the northwest European Continental Shelf from Geosat altimetry*, J. Geophys. Res., 95,* 3061–3068*, doi:*10.1029/JC095iC03p03061, 1990.

Zhang, Y.J., Stanev, E. V., and Grashorn, S.: Unstructured-grid model for the North Sea and Baltic Sea: validation against observations, Ocean Model., 97, 91–108, 2016.

Zhang, Y.J., Ye, F., Stanev, E.V., and Grashorn, S.: Seamless cross-scale modelling with SCHISM, (in revision) Ocean Model., 2016.

Zhang, Y., and Baptista, A. M.: SELFE: a semi-implicit Eulerian–Lagrangian finite-element model for cross-scale ocean circulation, Ocean Model., 21, 71-96, 2008.

Zhang, Y. J., Ateljevich, E., Yu, H. C., Wu, C. H., and Jason, C. S.: A new vertical coordinate system for a 3D unstructured-grid model, Ocean Model., *85*, 16-31, 2015.

Ocean Science
Discussions

Open Access

EGU

Figures and Tables.

D50 median sediment grain diameter (mm)	Sediment Grain Density (kg/m³)	Particles settling velocity (mm/s)	Surface erosion rate (kg/(m²*s))	Critical shear stress for erosion and deposition (N/m²)	Sediment Porosity
0.12	2650.0	8.06	0.016	0.15	0.4

Table 1: Characteristics of the sediment class used for the simulation

Ocean Science
Discussions

Open Access

EGU

Buoy	Number of comparisons	Mean of measurements	Bias	Root mean square error	Skill	Scatter index
H_s	-	(m)	(m)	(m)	-	(%)
old wave model version without wave breaking and with default wave growth parametrization						
Helgoland	247	1.44	0.17	0.47	0.79	30
Elbe	87	1.70	0.25	0.47	0.78	24
Westerland	248	1.15	0.35	0.62	0.64	44
improved wave breaking and modified wave growth in the wind input source term						
Helgoland	247	1.44	0.01	0.34	0.85	24
Elbe	87	1.70	0.08	0.35	0.83	20
Westerland	248	1.15	0.19	0.34	0.82	25
skill : reduction of variance, scatter index : standard deviation*100/mean of the measurements						

Table 2. H_s statistics during storm Xavier in the German Bight. The positions of buoys are shown in Fig. 1.
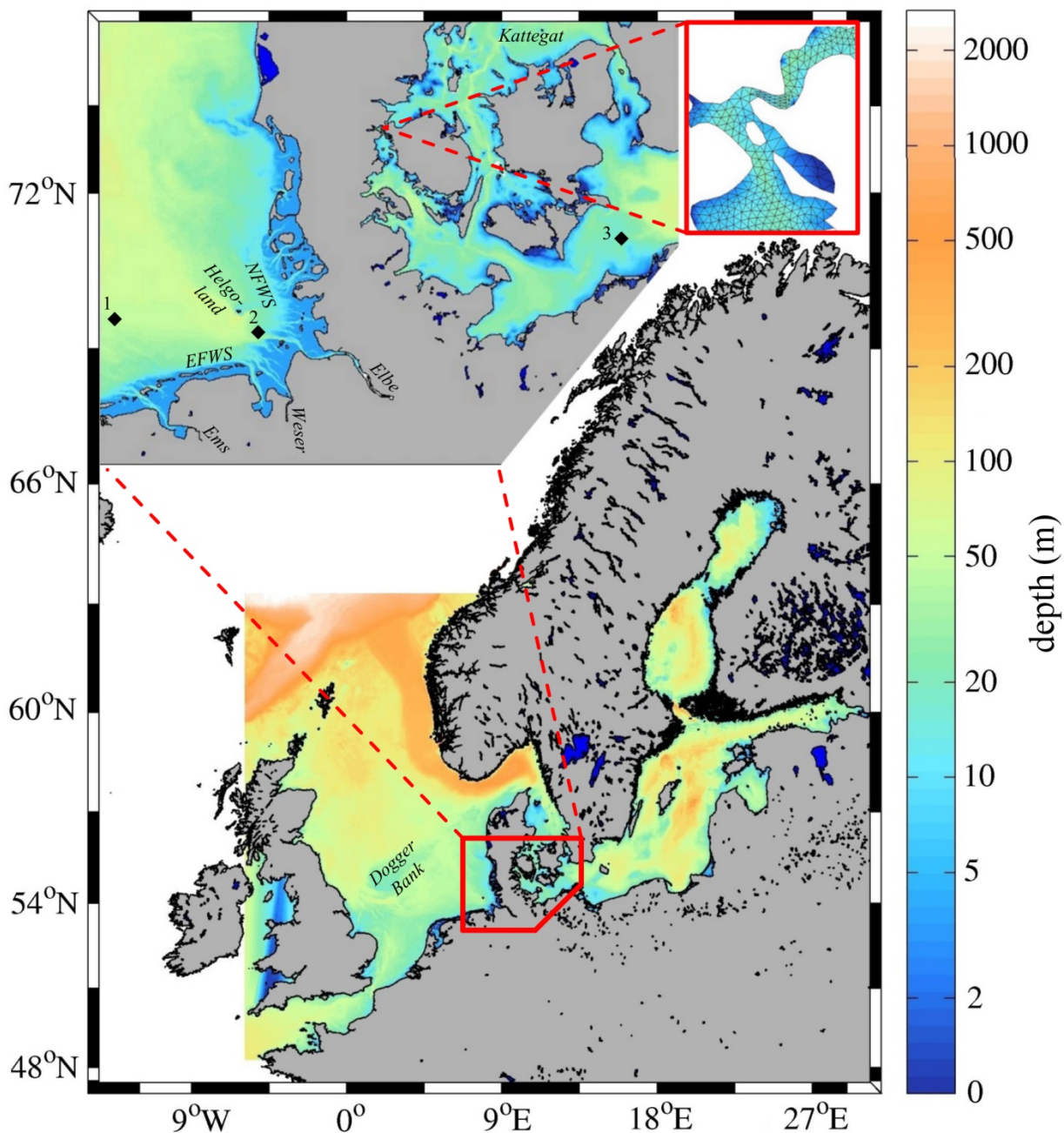
Fig. 1: Bathymetry of the North and Baltic Seas. The zoom in the upper-left corner shows the bathymetric details of the German Bight and of the straits connecting the Baltic to the North Sea. The smaller zoom in the upper-right corner illustrates how fine the resolution needs to be in order to resolve the straits (in this case the Little Belt). The rhombs identify the locations of the MARNET stations (1 – Ems, 2 – Elbe, 3 – Darss Sill).

a)

b)
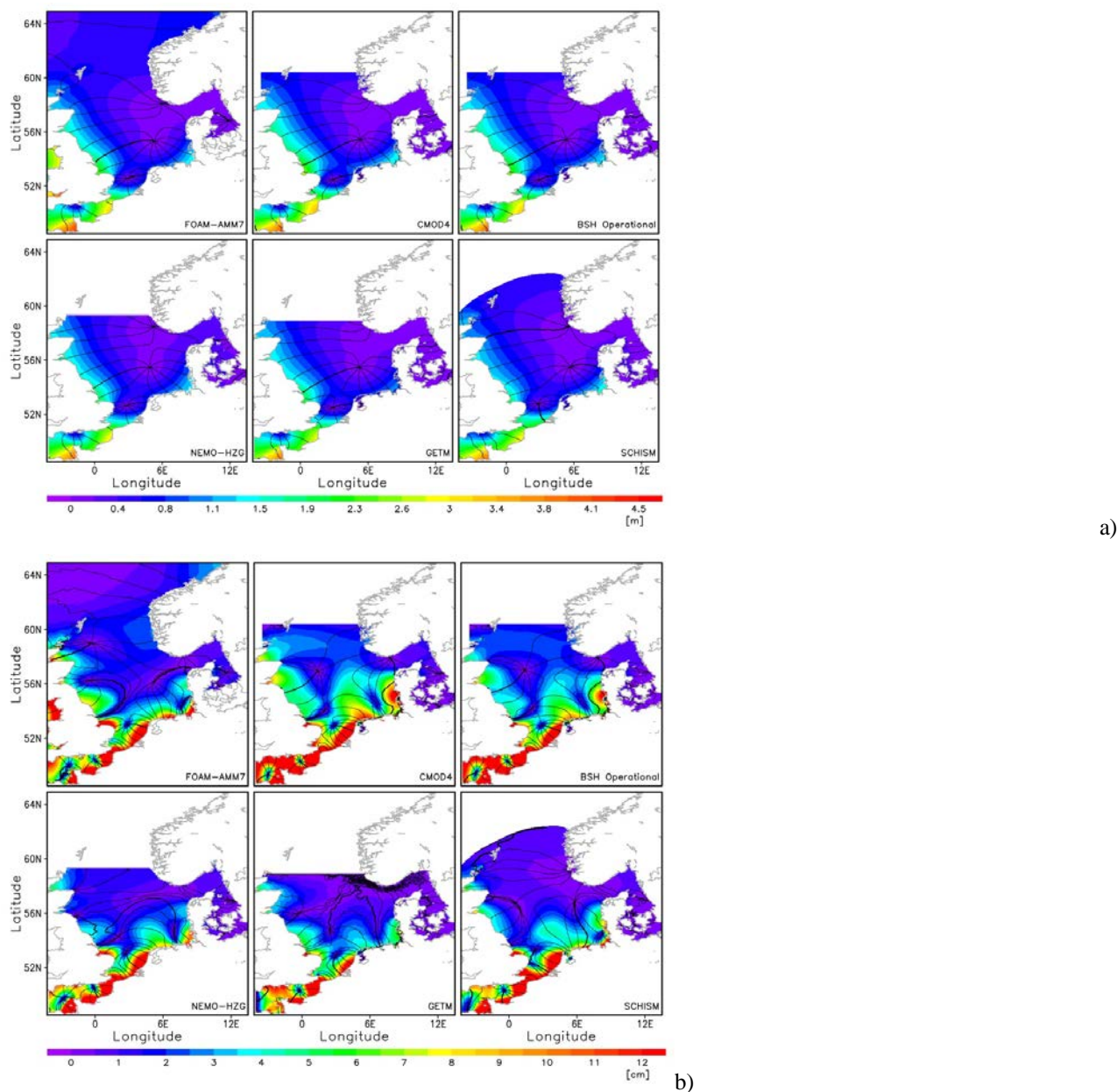
Fig. 2: Simulated M2 (a) and M4 (b) tidal amplitudes and phases from six different models operating in the North Sea.
The simulations using NEMO-HZG, GETM, SCHISM and BSHcmod are carried out at the HZG. Estimates for
FOAM-AMM7 and BSHcmod (operational) are derived from the freely-available data provided by the marine forecast
services (Met-Office) and BSH, respectively.
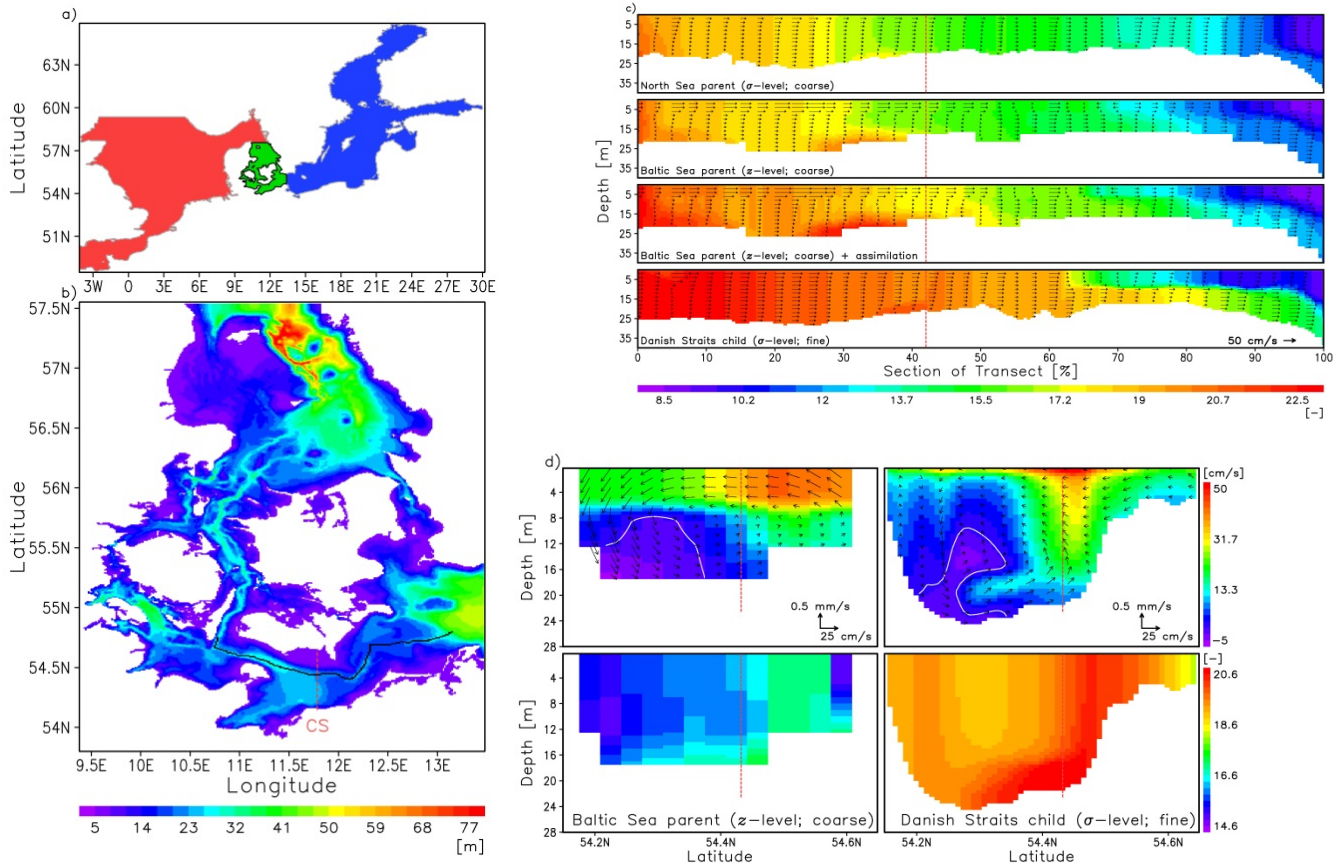
Fig. 3. (a) shows the individual model areas: red+green+blue-colors depict the coarse-resolution model area for the entire domain; red+green and green+blue are the areas for the coarse-resolution North Sea and Baltic Sea models, respectively. The coupling between the different models is performed over the green area, which is presented in (b) along with the bathymetry as seen in the fine-resolution nested model. Sections along which some results are analyzed (c and d) are also shown. (c) shows snapshots of velocities (vectors) and salinity (colors) from the different model nesting experiments (names are given in the individual panels) during an inflow period on the 16th September 2010. Data is shown for the long-channel transect (a, black line). (d) shows an across-channel section of velocity and salinity. The position of section is shown with the red line in (a).The position where the two sections sross is indicated by the vertical red lines in c and d.
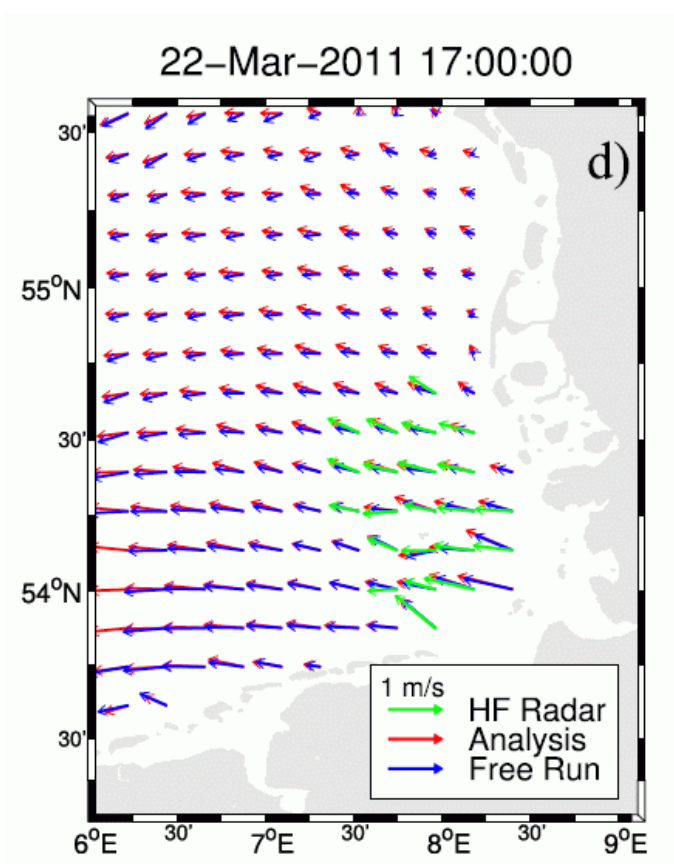
Fig. 4. Surface currents in the German Bight. The green arrows represent the HF radar measurement (not over the entire model area), the blue arrows are based on the free model run and the red arrows are the analysis.

5

Ocean Science
Discussions
Open Access

EGU
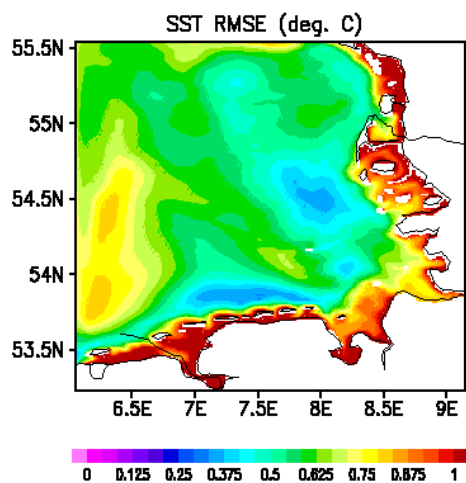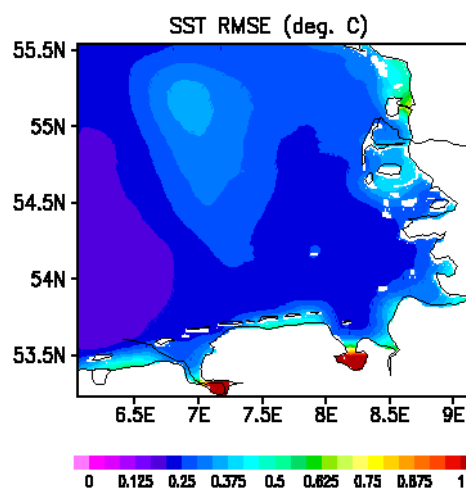
Fig. 5. (a) The RMSE between OSTIA SST and the numerical simulations from the free run of the German Bight model (see Annex 6.2) for 2011. (b) is the same but with assimilation of OSTIA SST data.

5

(a)

(b)

(c)
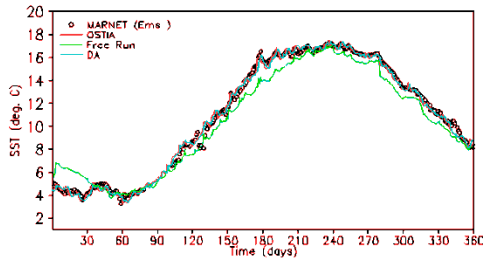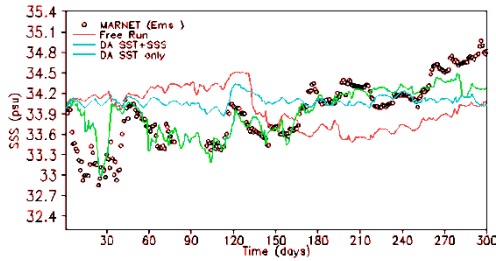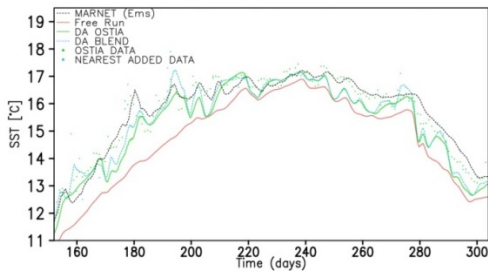
Fig. 6. Validation of the simulated with the German Bight model SST (a) and SSS (b) against the MARNET observations during 2011 for the Ems data station (see Fig. 1 for its position). Black circles are MARNET observations, the red line is the free run, the blue line corresponds to the case when only SST is assimilated, the green line shows the results when the assimilation of SST and SSS from Ferry box is added. (c) shows a zoom in time with higher resolution for temperature only for the warm part of year. Temporal resolution of the data is hourly and it is smoothed with an 24 hours running mean in order to filter out the daily cycle. The picture demonstrates the outcome of assimilating fine-resolution SST data (the different experiments and data are shown in the legend).

Ocean Science
Discussions
Open Access
EGU

a)   b)
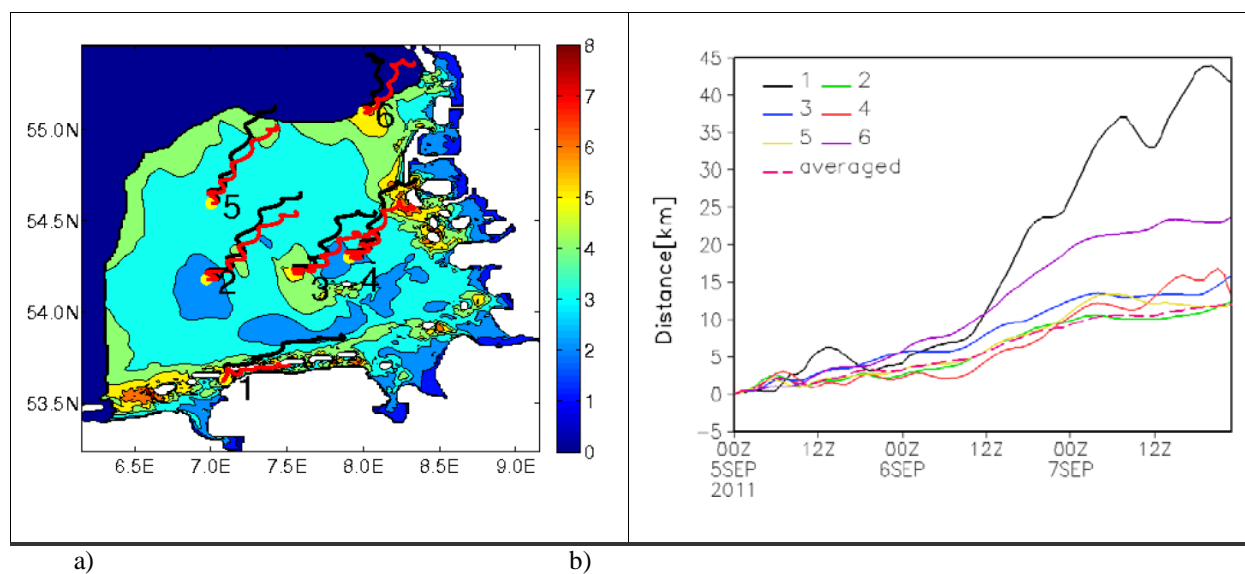
Fig. 7. (a) The displacement of Lagrangean particles. Black lines give the results from the model free run, red trajectories

5   visualize the results in the data assimilation run. Color coding gives the mean distance in km between position of Lagrangean

particles in the analysis and free run for September 2011 after 24h of integration. (b) Distance of drifting particles in the

assimilation run and the free run.

a)

b)

5

10

15
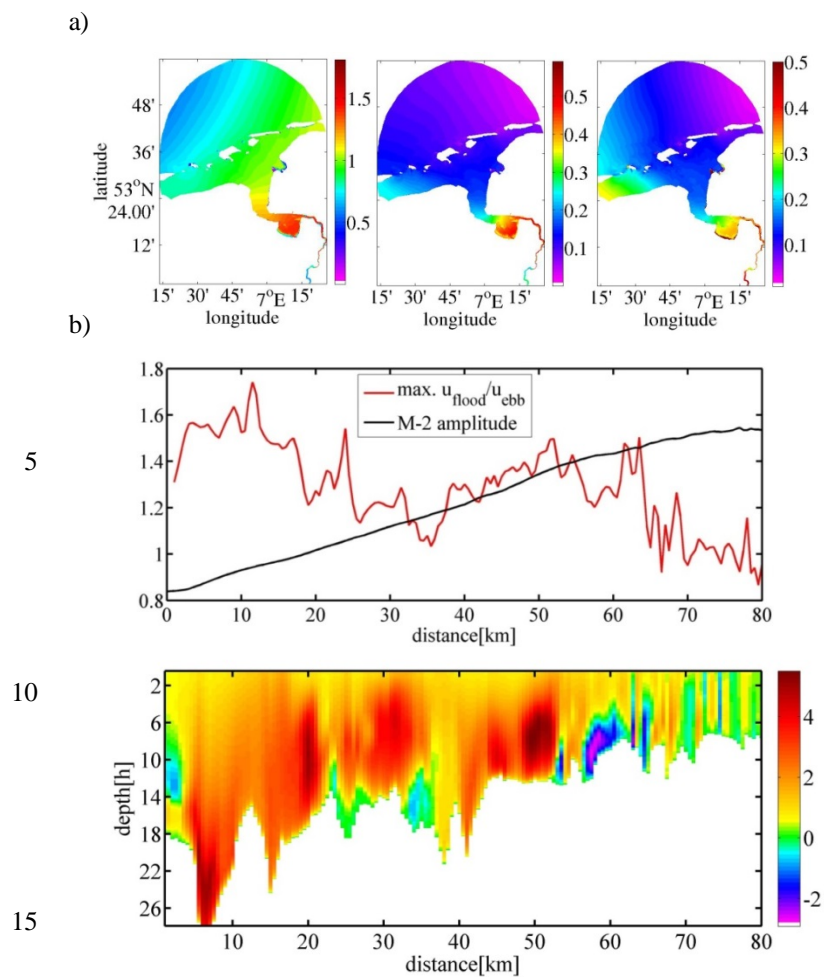
Fig. 8. (a) M2 (left), M4 (middle) and M4/M2 amplitude (right) simulated in the Ems Estuary. These constituents are computed using a tidal analysis of model data in October, 2013. (b) is the ratio between maximum flood and maximum ebb along-channel surface flow (tidal current asymmetry, red line) and the M-2 tidal amplitude [m] along the main estuarine channel(black line); (c) is the log(ratio) between the average flood and ebb eddy viscosity.
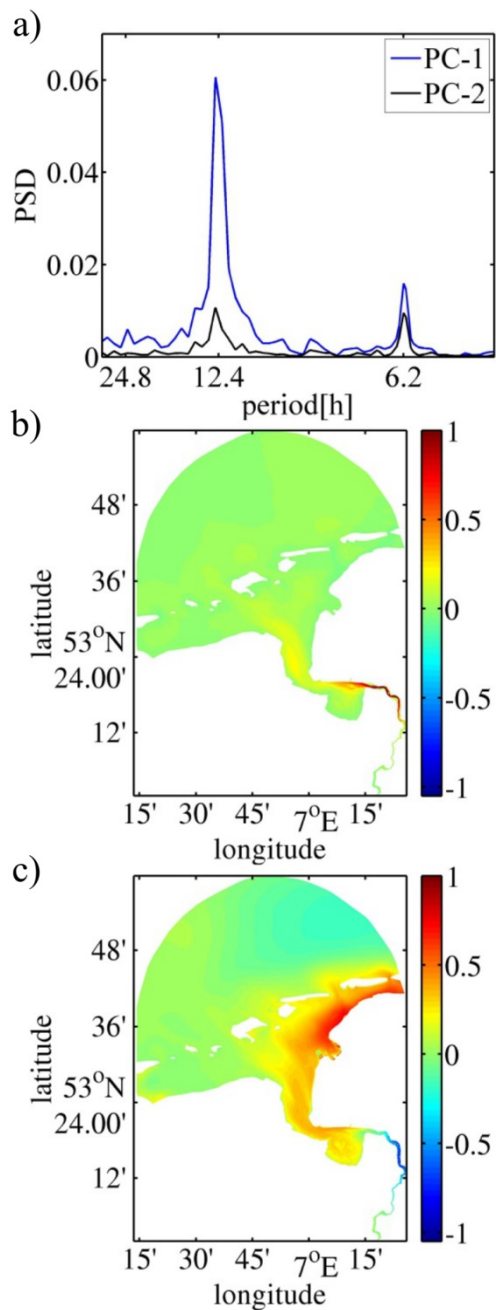
Fig. 9. The power spectral density of the PCs corresponding to the first two EOFs (a). The EOF decomposition is based on the 3D model outputs for salinity and is shown for the surface salinity. (b) and (c) are EOF-1 and EOF-2.

5

Ocean Science
Discussions

Open Access

EGU
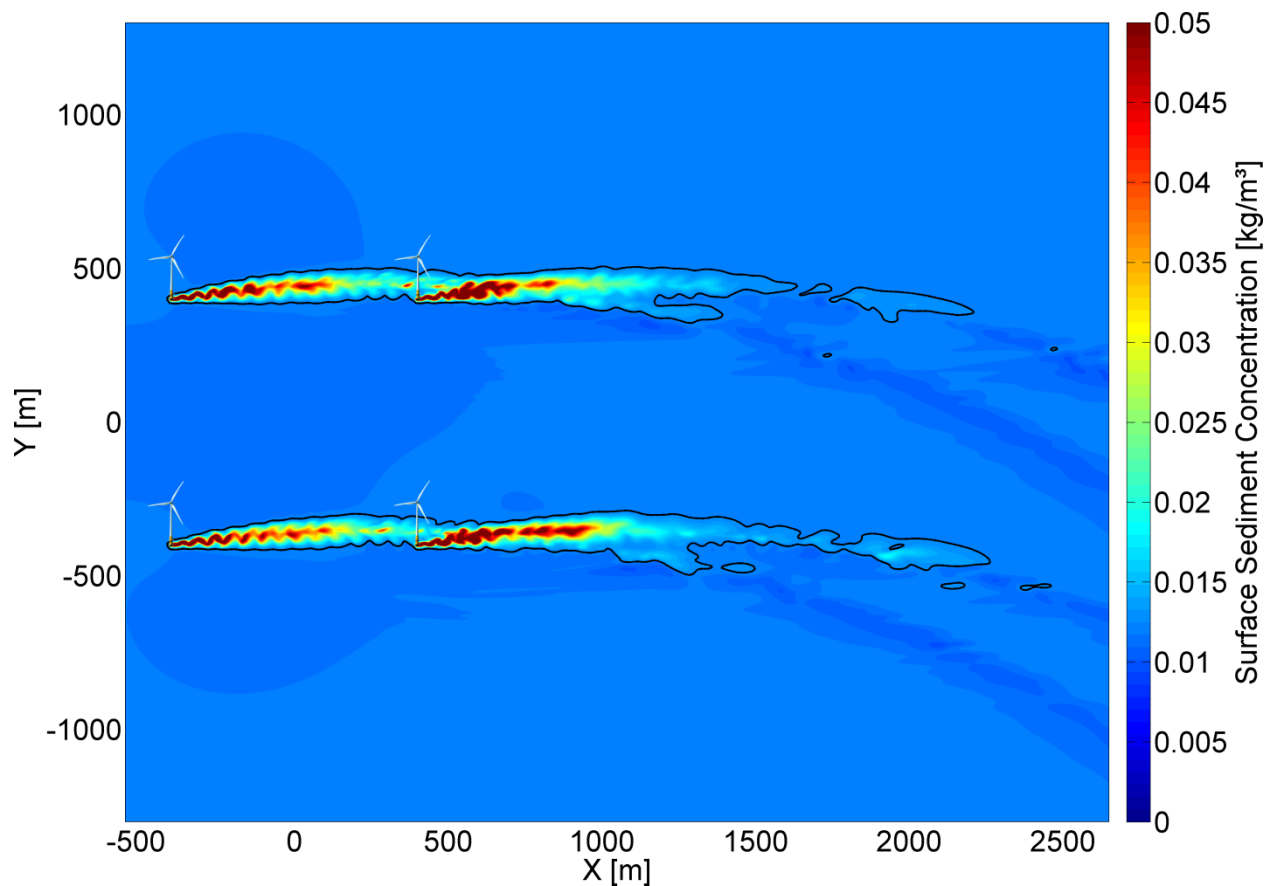
Fig. 10. Snapshot of surface sediment concentration for a circular basin with four bathymetric obstacles representing wind park turbine piles. This model setup is forced by a rotating M2-tide. The depth is 21.6 m and the highest resolution close to the piles is 1.5 m. An isoline is shown for 12.5 g/m³. The picture of the wind turbine piles was downloaded from https://commons.wikimedia.org/wiki/File:Off-shore_Wind_Farm_Turbine.jpg. The piles have been enlarged by a factor of 2 for a better presentation.

Ocean Science
Discussions

Open Access

EGU
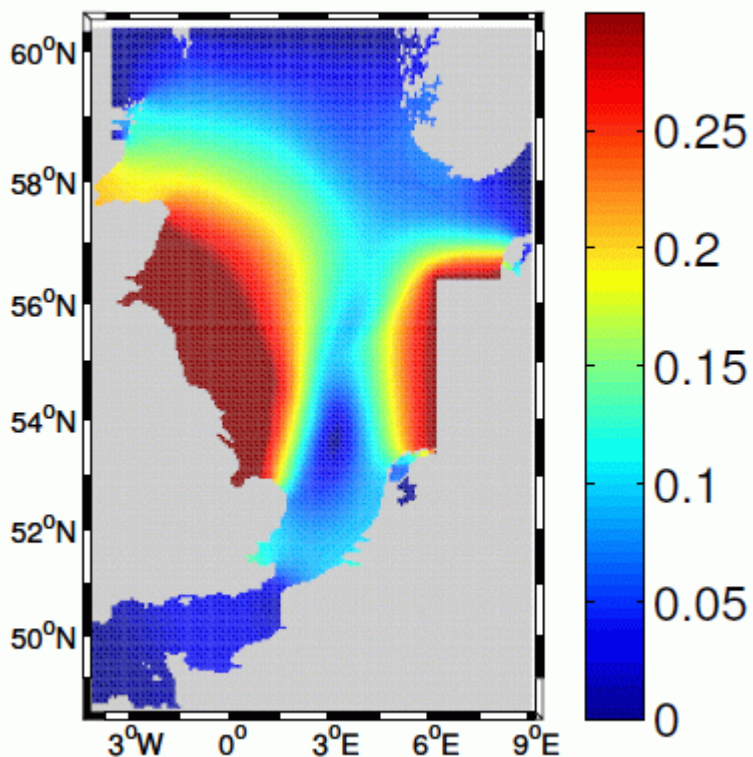
Fig. 11. This figure illustrated the impact of coastal boundary condition of a nested model on the North Sea dynamics. The model used was a two-dimensional linear barotropic model for the entire North Sea with 5 km resolution. It is solved in the spectral domain for the dominant M2 tide. A German Bight model with 1 km resolution is nested into the North Sea grid and the spectral model is solved in a two way nested configuration. The simplicity of this model allows its inversion, which enables relatively easy estimate of the influence of coastal boundary condition on the performance of the North Sea model (Schulz-Stellenfleth and Stanev, 2016). The figure originates from Schulz-Stellenfleth and Stanev (2016) and shows the standard deviation of elevation resulting from fully correlated perturbations with stdv 0.3 m along the German Bight border.
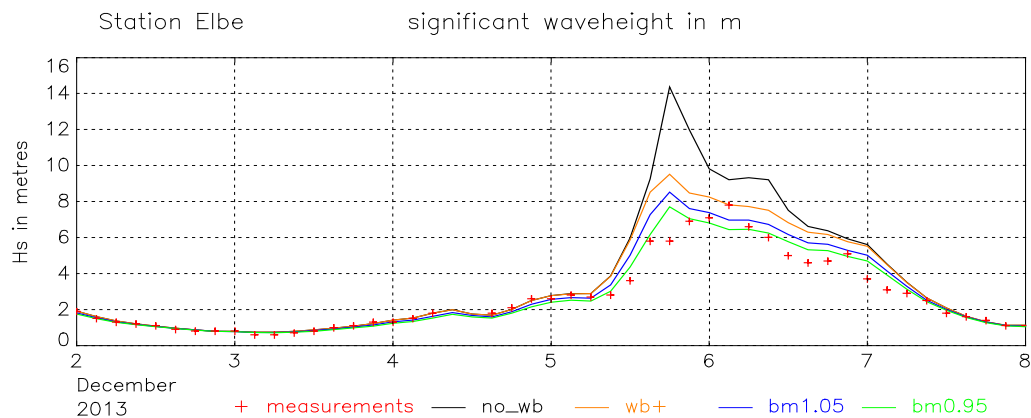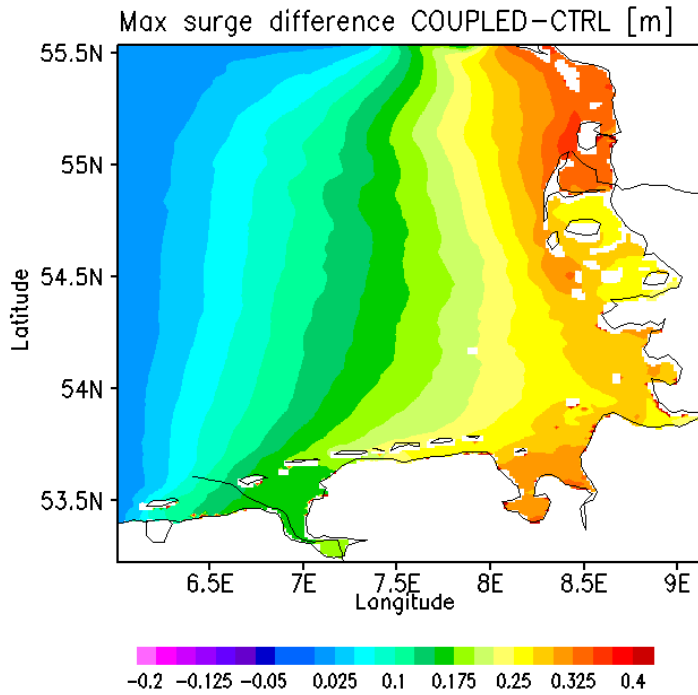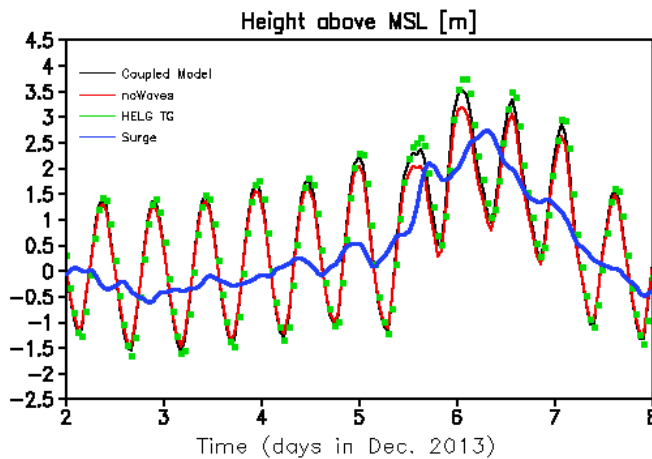
Figure 12. Time series of significant wave heights at Elbe station (see Fig. 1 for its position) during the storm Xavier (no_wb : run without wave breaking, wb+ : run with a new formulation for wave breaking, bm1.05 : run with a changed constant Betamax = 1.05 in the wave growth parametrization (default = 1.2), bm0.95 : run with Betamax = 0.95, the last two runs include wave breaking).

a)

b)

Fig. 13. (a) is the difference between sea surface elevation (SLE) between coupled wave-circulation model (WAM-GETM) and the circulation- only model (GETM) for the German Bight during the storm Xaver on 06.12.2013. (b) shows time series of Sea Level Elevation (SLE) in [m] at Helgoland tide gauge station. Black line: coupled wave-circulation model; red line circulation only model; green: tide gauge observations; blue line: the surge.